PŘÍRODOVĚDECKÁ
FAKULTA
Univerzita Karlova

BAKALÁŘSKÁ PRÁCE

Ondřej Groborz

Chelatující polymery pro léčbu hemochromatózy

Chelating Polymers for the Haemochromatosis Treatment

Vedoucí práce: Mgr. Martin Hrubý, Ph.D., DSc.

Konzultanti: Ing. Kristýna Kolouchová
Ing. Pavel Švec

Studijní program: Chemie

Studijní obor: Chemie

Praha
2019

Prohlašuji, že jsem tuto bakalářskou práci vypracoval samostatně a výhradně s použitím citovaných pramenů, literatury, dokumentace přístrojů a dalších odborných zdrojů. Při jejím vypracovávání byla použitá data získaná ve spolupráci s mými kolegy.

Prohlašuji, že jsem tuto práci ani žádnou její podstatnou část nepředložil k získání jiného či stejného akademického titulu.

V Praze dne 28. 5. 2019 Ondřej Groborz

Poděkování

Mé poděkování patří především Ing. Kristýně Kolouchové a Ing. Pavlu Švecovi za cenné rady, pomoc s interpretací dat a za velmi důkladnou korekturu práce. Dále bych chtěl poděkovat RNDr. Lence Polákové, Ph.D., za velkou pomoc měřením oxidativních vlastností materiálů; Ing. Jiřímu Trousilovi za měření *in vitro* cytotoxicity; RNDr. Janu Kučkovi, Ph.D. za pomoc při přípravě radiačně značeného polymeru; RNDr. Lence Loukotové, Ph.D. za pomoc při grafickém zpracování; Ing. Pavle Francové, Mgr. Petru Páralovi, Ph.D., Ing. Janu Krijtovi, Ph.D a RNDr. Luďku Šefcovi, CSc. za pomoc při *in vivo* experimentech a s interpretací jejich výsledků. Nakonec bych chtěl poděkovat svému školiteli Mgr. Martinu Hrubému, Ph.D., DSc. za vedení práce a za možnost pracovat na tomto projektu.

Bylo mi velkou ctí s nimi spolupracovat. Svou pomocí, radami a upomínkami umožnili vznik této práce, za což jsem jim velmi vděčný.

Děkuji i všem ostatním, všem přátelům, rodině, kolegům, učitelům, apod., kteří mě jakkoliv podporovali, poučili, inspirovali a měli se mnou trpělivost; i když se nejednalo zrovna o kontext této práce.

Tato práce byla spolufinancována z grantu Grantové Agentury České republiky (grant # 19-01438S).

Acknowledgement

I would like to thank Ing. Kristýna Kolouchová and Ing. Pavel Švec very much for their guidance, help with data interpretation and a very thorough thesis correction. I would like to thank RNDr. Lenka Poláková, Ph.D., for a great help with anti-oxidative properties analysis; Ing. Jiří Trousil for *in vitro* cytotoxicity analysis; RNDr. Jan Kučka, Ph.D. for his help with radio-labeling polymers with radioactive iodine; RNDr. Lenka Loukotová, Ph.D. for help with graphical design; Ing. Pavla Francová, Mgr. Petr Páral, Ph.D., Ing. Jan Krijt. Ph.D. and RNDr. Luděk Šefc, CSc. for help with *in vivo* experiments and the data interpretation. Last but not least I would like to thank my tutor Mgr. Martin Hrubý, Ph.D., DSc. For his guidance, help and the opportunity he gave me to work on this project.

It has been an honour to work with them. Their help and advice were incredibly useful, and I am very grateful for them.

I would like to thank everyone else, all friends of mine, my family, my colleagues, my teachers, etc. who have supported me in any way, edified me, inspired me and had patience with me; even if they were not directly connected to this thesis.

The authors acknowledge financial support from the Czech Science Foundation (grant # 19-01438S).

Chelatující polymery pro léčbu hemochromatózy

Autor: Ondřej Groborz

Vedoucí práce: Mgr. Martin Hrubý, Ph.D., DSc.
Konzultanti: Ing. Kristýna Kolouchová
Ing. Pavel Švec
Ústav makromolekulární chemie Akademie věd České republiky, v.v.i

Abstrakt

Hemochromatóza je skupina dědičných onemocnění, jež je charakterizována toxickým nahromaděním železa v orgánech. To může vést k orgánové toxicitě a nevratnému poškození. V současné době existuje pouze málo schválených léčebných postupů, z nichž všechny mají závažné nežádoucí účinky.

V této práci navrhujeme nové paradigma léčby: nerozpustné a tedy biologicky nevstřebatelné polymery by vytvářely stabilní komplexy s železnatými či železitými ionty v gastrointestinálním traktu, čímž by snížily biologickou dostupnost železa. Nerozpustnost těchto polymerů brání jejich vstřebání a tím zamezuje vzniku systémové i orgánové toxicity.

Bylo připraveno několik polymerů s kovalentně vázanou selektivní chelatační skupinou. Na základě dat získaných *in vitro* a *in vivo* byly vybrány ty chelatující skupiny, které byly dostatečně účinné pro případné klinické aplikace. Polymery vykazují zanedbatelnou vstřebatelnost, zanedbatelnou toxicitu, mají velmi vhodnou kinetiku *in vitro* chelatace železnatých i železitých iontů a mají prokazatelný terapeutický účinek na *in vivo* modelu. Proto by mohly být použity jako terapeutikum nové generace pro léčbu hemochromatózy a/nebo nemocí s podobnou patofyziologií.

Klíčová slova: hemochromatóza; železo; metabolismus železa; inhibitor příjmu; příjem železa; chelátor, polymer; léčba; terapie

Chelating Polymers for the Haemochromatosis Treatment

Author: Ondřej Groborz

Tutor: Mgr. Martin Hrubý, Ph.D., DSc.
Advisors: Ing. Kristýna Kolouchová
Ing. Pavel Švec
Institute of Macromolecular Chemistry, Czech Academy of Sciences

Abstract

Haemochromatosis is a group of hereditary diseases which are characterised by toxic accumulation of iron in parenchymal organs, leading to organ toxicity and irreversible damage. Currently, there are only a few approved medications for this disease, yet all of them possess severe side effects.

Herein, we have proposed a new paradigm for treatment: insoluble polymers with negligible systemic biological availability would form stable complexes with iron ions in the gastrointestinal tract, hence decreasing biological availability of iron. The insolubility of polymers prevents them from being absorbed into the organism in the first place while having no systemic side effects or toxicity. We have prepared polymers with several covalently bound iron-chelating ligands and based on the biological data we selected the most successful chelators for possible future applications. These polymers exhibited negligible resorbability and toxicity, superior *in vitro* iron chelating activity and their efficacy was proven in an *in vivo* model. Therefore they could be used as a next-generation polymer therapeutics for haemochromatosis and/or other diseases of similar pathophysiology.

Key words: haemochromatosis; hemochromatosis, iron overload iron; iron metabolism; uptake inhibitor; iron uptake; chelator; polymer; polymer treatment; treatment; therapy

Table of content

1. Introduction

1.1 Iron homeostasis and haemochromatosis

Iron is essential for a proper body function. Homeostatic balance requires only only 1 to 3 mg of absorbed iron per day to offset losses from desquamated cells. However, there are no known regulated means of iron excretion, and therefore dietary iron absorption (primarily from duodenal enterocytes) is the only way of regulation. (Simpson R.J., 2009)

Haemochromatosis is a group of hereditary diseases characterized by toxic accumulation of iron in the organism. It can be caused by mutations in any gene that limits iron entry into the blood (Pietrangelo, 2010) (Brissot P., 2008). Most of them have the similar pathophysiology – inadequate or ineffective hepcidin-mediated down-regulation of ferroportin, which is an important membrane iron transporter (Fleming R.E., 2012) (Kondo H., 1988). As a result, the body takes in significantly more iron than it needs, leading to accumulation in the long term. There are four major cell types that regulate the intake of iron: duodenal enterocytes, erythroid precursors, reticuloendothelial macrophages and hepatocytes (Fleming R.E., 2012). Worldwide prevalence of the most common haemochromatosis type 1 is 1:200-400 and clinical presentation usually occurs in middle age (Pietrangelo, 2010) (Eijkelkamp E.J., 2000). Progressive accumulation of iron occurs mostly in the liver, pancreas, joints, skin, heart and the gonadotrophin-secreting cells of the pituitary (Griffiths, 2011). Without a treatment, iron overload in the organs causes the production of reactive oxygen species, which can damage intracellular structures leading to the disease manifestations with increased pigmentation, hepatic fibrosis, diabetes mellitus, arthropathy, cardiomyopathy and hypogonadotropic hypogonadism (Griffiths, 2011) (Pietrangelo, 2010). Untreated haemochromatosis patients have a significantly increased risk of liver cirrhosis and hepatocellular carcinoma. (Adams P.C., 2007)

1.2 Current treatment

Currently, the main approach of haemochromatosis treatment is the phlebotomy (Sood R., 2013). This method involves the removal of 450-500 mL of blood once or twice a week until iron levels reduction to required serum levels (Flaten T.P., 2012). However, there is only a limited knowledge of how to assume the endpoint of therapeutic phlebotomy or the frequency of the maintenance therapy (Simpson R.J., 2009). An alternative to the phlebotomy (due to intolerance or contraindication) is iron chelators therapy (Simpson R.J., 2009) (Brissot P., 2011). The traditional chelator deferoxamine (Desferal®) must be administered intravenously or subcutaneously because of its rather poor absorption from the gastrointestinal tract. The main obstruction of this method is severe side effects including ophthalmic and auditory toxicity, increased risk of bacterial and fungal infections, changes in blood histology, allergic and skin reactions, and pulmonary, renal and neurological damage (Galy B., 2008). *Per os* administrable FDA-approved iron chelators deferiprone (Ferriprox®) and deferasirox (Desirox®, Exjade®) are effective, but cause severe side effects as well, such as agranulocytosis, hepatic fibrosis and renal toxicity (Roberts D.J., 2007) (Henter J.I., 2007) (Cappellini M.D., 2006) (European Association For The Study Of The Liver, 2010). Low-iron diets are also recommended for iron level maintenance, nevertheless, it is of limited efficacy due to the omnipresence of iron (as an essential element for any organism) in the diet. (Simpson R.J., 2009)

1.3. Chemistry of iron

Iron is an abundant metal, which account for roughly 5 % of the Earth's crust (Morgan, et al., 1980). Its chemistry is well known, the most common oxidative states of iron are Fe^0, Fe^{2+}, and Fe^{3+}.

The Fe^{3+} ions are rather hard acid (according to HSAB theory) (Pearson, 1963). In aqueous solution they forms a pink to pale-violet hexaaquairon(III) ions. These can deprotonate easily (pK_{a1}= 3.05 and pK_{a2} = 3.26) yielding pentaaquahydroxoiron(III) and tetraaquadihydroxoiron(III) ions, respectively with a rusty to orange colour. (Greenwood, et al., 1997) These ions easily eliminate water forming insoluble oligomers and polymers, hence an acidic pH is required in order to prevent deprotonation and subsequent precipitation. Fe^{3+} ions are rather oxophilic, meaning they coordinate easily to oxygen *e.g.* in phosphates, acetylacetonate anion, citrate, oxalates or catechol. Rather stable complexes were described with cyanide or thiocyanate ligands. Vast majority of Fe^{3+} complexes are high-spin, only a few low-spin complexes are known (e.g. $[Fe(CN)_6]^{3-}$). Most common geometry of these complexes is octahedral. (Greenwood, et al., 1997) (Remy, 1972)

The Fe^{2+} ion forms pale-green hexaaquairon(II) ions in aqueous solutions. They are significantly softer acids than Fe^{3+} ions (HSAB). These solutions are rather prone to oxidation by the atmospheric oxygen, the susceptibility to oxidation is highly dependent on the coordinated ligands (out of inorganic ligands double sulphates, *e.g.* $(NH_4)_2Fe(SO_4)_2$, are one of the least prone to the oxidation). (Greenwood, et al., 1997) (Schilt, 1962) Electrode potentials of various complexes can be seen in Table 1. Fe^{2+} forms stable complexes with many ligands, most of them are high-spin, however some very stable low-spin complexes are known (*e.g.* $[Fe(CN)_6]^{4-}$, $[Fe(bipy)_3]^{2+}$ or $[Fe(phen)_3]^{2+}$). Most complexes have octahedral geometry (*e.g.* $[Fe(CN)_6]^{4-}$ or $[Fe(cat)_3]^{4-}$) but tetrahedral complexes of $[FeX_4]^{2-}$ (where X can be Cl, Br, I or NCS) are known. (Greenwood, et al., 1997) (Remy, 1972)

Complex reaction	E^0 (V)
$[Fe(phen)_3]^{3+} + e^- \rightleftharpoons [Fe(phen)_3]^{2+}$	1.12
$[Fe(bipy)_3]^{3+} + e^- \rightleftharpoons [Fe(bipy)_3]^{2+}$	0.96
$[Fe(H_2O)_6]^{3+} + e^- \rightleftharpoons [Fe(H_2O)_6]^{2+}$	0.77
$Fc^+ + e^- \rightleftharpoons Fc$	0.40
$[Fe(CN)_6]^{3-} + e^- \rightleftharpoons [Fe(CN)_6]^{4-}$	0.36
$[Fe(C_2O_4)_3]^{3-} + e^- \rightleftharpoons [Fe(C_2O_4)_2]^{2+} + C_2O_4^{2-}$	0.02
$[Fe(edta)_3]^- + e^- \rightleftharpoons [Fe(edta)_3]^{2-}$	–0.12
$[Fe(quin)_3] + e^- \rightleftharpoons [Fe(quin)_2] + quin^-$	–0.30

Table 1: Standard reduction potentials of various iron complexes at 25 °C in acidic aqueous solution. (Greenwood, et al., 1997) (Bard, 1985)

There are many biologically important iron complexes, *e.g.* heme which has protoporphyrine ring coordinated to the Fe^{2+} ion, is an essential molecule and a coenzyme in haemoglobin, myoglobin, cytochromes and other proteins. If the central Fe^{2+} in the haemoglobin is oxidised, the protein loses its primary function and is then referred to as methemoglobin. Heme analogue with Fe^{3+} and with bound chloride is called hemin and with bound hydroxide is called hematin. So-called iron-sulphur clusters (also known as Fe-S clusters) can be found in several enzymes (*e.g.* in nitrogenase or aconitase). In these clusters various number of iron atoms is bound to a various number of cysteine sulphur from the

protein. These clusters have cubic (4Fe-4S or 3Fe-4S) or di-tetragonal (2Fe-2S) shape and have catalytic oxidative properties. (Greenwood, et al., 1997)

1.4. Iron speciation in the food

There are three common forms of iron in the food. Vast majority of the iron in the food occurs in oxidative state Fe^{3+}; a minority (since it is oxidised easily by the omnipresent oxygen) occurs in Fe^{2+} state and in some diets (mainly in meat a portion of the total iron content occurs in heme-chelated form. There is a natural equilibrium between Fe^{3+} and Fe^{2+} oxidative states, these ions can be oxidised/reduced by the food. (Peters, et al., 1992)

Only Fe^{2+} and heme forms of iron are biologically available. Heme-chelated iron is taken up easily from the gastrointestinal tract. The Fe^{2+} is also relatively easily taken up, but the most common form of iron Fe^{3+} cannot be absorbed and needs to be reduced before the absorption. (Peters, et al., 1992)

Increased uptake of ascorbic acid, lactate or other reducing agents leads to increased Fe^{2+} concentrations in the gastrointestinal tract leading to increased biological uptake. On the other hand it has been proven that increased uptake of molecules which form a stable complex with iron ions (*e.g.* phytates or tannic acid) leads to a decreased iron uptake. (Bryszewska, 2019)

1.5. Suspension polymerisation

Suspension polymerisation is a type of free radical polymerisation that enables preparation of round polymer particles. Both monomers and the initiating agent (usually AIBN or dibenzoyl peroxide) need to be soluble in a hydrophobic organic solvent (also knows as porogen, *e.g.* toluene or cyclohexanol), but must not be soluble in the aqueous layer. The aqueous phase contains a terminating agent (typically sodium nitrite) and another compounds to modify the surface tension or viscosity (such as carboxymethyl cellulose or polyvinylpyrrolidone). (Lima, et al., 1997)

The reaction mixture is then stirred vigorously in order to disperse the organic phase within the aqueous phase and heated to start the polymerisation. Therefore, radical polymerization proceeds readily in the organic phase forming microbeads while being terminated in the aqueous phase, which prevents the irreversible aggregation of beads due to cross-polymerization. If the polymer, unlike the monomers, is insoluble in the organic solvent (*e.g.* due to cross-linkage), it precipitates out of the solution forming a macroporous structure. After the polymerisation the beads need to be washed thoroughly to eliminate any unreacted monomers and other soluble compounds. (Lima, et al., 1997)

1.6. Fourier-Transform Infrared Spectroscopy (FTIR)

Fourier-transform infrared spectroscopy is a technique used for obtaining the infrared spectrum of a compound of interest.

The infrared spectroscopy measures how much infrared radiation (wavenumber range from 10 to 12800 cm^{-1}) a particular sample absorbs. This absorbed energy correspond to transfer between vibrational and rotational energy states of the molecule. This range can be further divided to the near-infrared region (4000 to 12800 cm^{-1}), mid-infrared region (200 to 4000 cm^{-1}) and far-infrared region (50 to 200 cm^{-1}). The most useful region for compound structure determination is the mid-infrared region. It can be further divided into region 1500 to 4000 cm^{-1} where functional groups and moieties can be represented with their specific

vibrational signals, and region 500 to 1500 cm^{-1}, is the so-called fingerprint region. The fingerprint region contains peaks which are usually complicated to evaluate and they are used as a specific fingerprint of a certain molecule. (Worsfold, 2019)

In FTIR spectroscopy, a radiation source generates the entire mid-infrared spectrum of radiation. The beam then enters Michaelson interferometer, where certain wavenumbers are eliminated via an interference. The beam then enters the sample chamber, where it is partially absorbed, reflected or deflected. The residual transmitted light then enters the detector, where the intensity is measured. This process is performed multiple times, the adjustment of Michaelson interferometer causes different wavenumbers to be eliminated, which allows us to measure the entire spectrum. Moreover, his process can be automatized allowing the entire spectrum to be measured rather quickly. The data is then processed via the Fourier transform by a computer to get an IR spectrum. The advantage of the FTIR technique is that it allows obtaining the measured spectrum rather quickly in a range of seconds to minutes. (Griffiths, 1983)

1.7. Solid State Nuclear Magnetic Resonance (ssNMR)

Solid state nuclear magnetic resonance (ssNMR) is a technique of measuring NMR spectrum of solid samples. It gives information about both the chemical structure as well as mobility and flexibility of functional groups. Unlike liquid NMR samples or samples dissolved in a solution, solids have anisotropic dipolar interactions, quadrupole interactions and chemical shift (liquids and solutions are considerably less anisotropic in liquid phase due to the rotation of molecules at common temperatures of measurement). All these effects cause that solids have very broad peaks in NMR. Nevertheless, this can be avoided if the sample rotates at a high frequency, usually from 1 kHz to 130 kHz (for ^{13}C) under the so-called magic angle, approximately 54°44’ (Magic angle spinning, MAS). (Hennel, et al., 2004) This technique then gives rise to reasonably narrow peaks, which are easier to interpret. Higher frequencies of rotation give rise to narrower spectrum and suppress unwanted artefacts, but on the other hand, they are more hardware demanding and are very prone to sample explosion. The most common nucleus to be measured by this technique is ^{13}C since ^{1}H spectra are rather hard to interpret due to the width of NMR peaks even at very high rotation frequencies. (Hennel, et al., 2004)

In addition, the NMR can be measured with a cross polarisation (CP) technique, which takes advantage of both the ^{1}H being more relatively abundant than the ^{13}C and the ^{1}H having a higher Larmor frequency than the ^{13}C (both effects result in higher ^{1}H NMR sensitivity). The ^{1}H can be excited with a radiofrequency pulse and then the polarisation is transferred to the ^{13}C using a transfer pulse sequence. The signal is afterwards detected from the ^{13}C nuclei. The advantage of this technique is that it can have significantly higher sensitivity than a simple ^{13}C NMR for some samples and can have a faster repetition rate; the disadvantages are that this technique is more hardware demanding and that the intensity of the signals is distorted; hence a simple integration of NMR signals cannot be used for quantification. (Hennel, et al., 2004)

1.8. Atomic Absorption Spectroscopy (AAS)

Atomic absorption spectroscopy is an analytical technique for quantitative determination of element concentration within the sample.

A known volume of the sample dissolved in a solution is injected into an atomizer (most commonly a flame atomizer or electrothermal atomizer). In this atomizer a sample is vaporised; a beam of radiation (typically the source is a hollow cathode tube lamp made out of the same metal as the one investigated) is passed through this vapour of sample and it is partially absorbed. Every element has its own unique set of absorbed radiation wavelengths. The light is then passed to a monochromator and then to a detector which measures the spectrum. The absorption of the radiation from the radiation source is directly proportional to both the volume of injected sample and the concentration of the element within the sample, meaning the concentration can be calculated using the Lambert-Beer law. An external calibration (preferably one with the same matrix as the sample) is required for determination of the concentration-signal characteristic. (Fernández, et al., 2019) (Worsfold, 2019)

1.9. Static Light Scattering (SLS) and Multi-Angle Light Scattering (MALS)

Static light scattering (SLS) is a technique that measures the intensity of light scattered by a liquid sample to obtain the average molecular weight and radius of gyration (R_g) of macromolecules or particles present in the sample. Static light scattering uses a high-intensity monochromatic light (usually a laser) beaming through the liquid sample in a glass cuvette. The polymer solution (or suspension) can be prepared in multiple concentrations and for every sample the intensity of scattered light is measured in one or several angles (Multi-Angle Light Scattering – MALS). (Debye, 1944)

The detector must be normalized before the measurement. The normalisation is done by using a standard, typically pure toluene. . Data analysis is afterwards performed using Zimm plot. SLS methods give us information about the size of the measured polymer or polymer assemblies but also information about shape or branching, which makes it a particularly useful method in polymer chemistry. (Zimm, 1948)

1.10. Scanning Electron Microscopy (SEM)

Scanning electron microscopy is a technique which uses beams of electrons for sample image construction. Some electrons from this beam can be backward scattered, absorbed, transmitted or cause a secondary electron emission. The secondary emissions can be detected and interpreted using software to construct an image of the surface of the sample. This technique gives a detailed image with a resolution of less than 1 nm. (McMullan, 1953)

Samples, however, need to be conductive; otherwise, the absorbed charge would repel the electron beam, thus interfering with the measurement. In conductive samples, the charge can be drained and the interference can be limited. Non-conductive samples need to be coated with a small layer of metal, usually gold or platinum. In order not to damage or alter the surface of the sample a metal-vapor technique can be used, which deposits only a few atoms wide layers of metal. Alternatively, the sample can be exposed to vapours of volatile reactive compounds of highly conductive metals (such as osmium tetroxide), which upon decomposition forms a very thin and uniform layer of metal on the surface of the sample. (McMullan, 1953)

1.11. Single-Photon Emission Computed Tomography (SPECT)

Single-photon emission computed tomography (SPECT) is a useful non-invasive technique used for imaging in medicine and research. For the imaging in medicine a compound with a known biological distribution (most notably sestamibi (Cardiolite®) or tetrofosmin (Myoview®) and others) labelled with gamma rays emitting nuclide (most frequently ^{99m}Tc; ^{75}Se, ^{111}In, ^{123}I, ^{131}I, ^{133}Xe, and ^{201}Tl are also in clinical use; other nuclides such as ^{57}Co, ^{51}Cr, ^{67}Ga, and ^{125}I are sometimes used in research) (Hála, 2013) is administered to a patient's or test subject's body. Upon the administration, the compound is accumulated in tissues of interest (sestamibi, for example, accumulates in the myocardium, parathyroid glands and in breast cancer nodules). The present nuclides undergo a nuclear decay after which they emit gamma rays, which can be detected by the SPECT machine (gamma camera). The software subsequently reconstructs a 3D image of the biological distribution of the compound of interest revealing any possible abnormalities, such as tumours. (Kupka, et al., 2007) (Navrátil, et al., 2005)

The SPECT can also be used for determination of the biological distribution of new compounds with unknown biological distribution, on the condition that they can be labelled with a gamma-ray-emitting nuclide.

1.12. Computed Tomography (CT)

Computed tomography (CT) is an important non-invasive diagnostic technique used for imaging in medicine and research. It is based on taking a great number (can be as large as 120) of X-ray scans of the patient from various angles and then using software to reconstruct a 3D model of the patient's body. Since bones and teeth absorb X-ray photons rather well, this method is suitable for bone and teeth imaging, but with state-of-the-art detectors, it can be successfully used for soft tissues imagining as well. (Herman, 2010) (Navrátil, et al., 2005)

It is possible to fuse the hardware of SPECT and CT together forming a SPECT-CT scanner and to acquire both SPECT and CT scans of a patient or a test subject. SPECT image gives us information about the biological distribution of a compound of interest (molecular imaging) and the CT gives us a detailed spatial and anatomical information. The addition of CT to SPECT also allows more accurate attenuation correction of the photons by overlying tissues and organs. (Kupka, et al., 2007)

1.13. Inductively Coupled Plasma-Mass Spectroscopy (ICP-MS)

Inductively Coupled Plasma (ICP) is an analytical method for detection of ion (mostly used for metal ions) in very low concentrations sometimes as low as parts per trillion (ppt).

A known volume of the sample is dispersed in an atmosphere of a non-reactive gas (usually a noble gas, *e.g.* helium or argon). This mixture then enters a chamber, where it is heated to 6,000 to 10,000 K via a high frequency induction. Under these conditions all compounds are atomised, ionised and accelerated in the direction of the detection chamber. (Jervis, et al., 1991)

These ions then need to be separated and analysed. The separation can be conveniently done by the mass spectroscopy (MS) methods. These methods use magnetic and electric fields to separate and ions based on their m/z ratio (where m is mass of the ion and z is its charge). Most common type of detector to be used for ICP-MS tandem is

the so-called quadrupole detector or less commonly an ion trap detector. These detectors apply an oscillating electric field of a known frequency to modify the trajectory of all ions. Only the ions with the desired m/z ratio are subsequently transferred though the detector without a collision; the rest of the ions collide with the walls or the electrodes of this detector chamber. These ions are then captured by a conductive material and they are quantified by the charge they deposit on this conductive material. The oscillation frequency can be changed and a new group of ions can be detected; by repeating this process an entire spectrum is measured. (Becker, 2002)

2. Aim

The aim of this thesis will be to investigate a new paradigm of treatment of haemochromatosis and/or any other diseases which cause increased iron accumulation in the body.

1) A cross-linked carrier polymer poly(glycidyl methacrylate) will be prepared into microscopic macroporous spheres. The size and shape of the spheres will be determined.

2) These spheres will be modified with selectively chelating moieties. These moieties will be designed to have high chelating capacity, fast *in vitro* kinetics of Fe^{2+} and Fe^{3+} ions absorption and high selectivity. All these properties will be tested *in vitro* at different pH.

3) *In vitro* toxicity (cytotoxicity) will be determined.

4) The polymer will be traced with a radioactive nuclide and the biodistribution will be analysed using PET/SPECT. *Ex vivo* biodistribution will be analysed (a proof of non-absorbability).

5) The efficacy of the polymer-based treatment will be analysed.

6) The safety of a daily sub-chronic therapeutic administration will be determined. A histology will be used to detect any pathophysiology of the gastrointestinal tract or any other organ.

3. Experimental Section

3.1. Materials

The human insulin solution (recombinant, BioXtra) was purchased from Sigma-Aldrich Ltd. (Prague, Czech Republic). Amphotericin B (250 μg/mL), Dulbecco's Modified Eagle Medium (DMEM, high glucose, GlutaMAX™), DMEM (powder, without $NaHCO_3$), fetal bovine serum (FBS, heat-inactivated) and Penicillin-Streptomycin (10,00 U/mL) were purchased from Life Technologies Czech Republic Ltd. (Prague, Czech Republic).

1,10-Phenanthroline-5-amine (ultrapure) was purchased Puralab s.r.o, (Běchovice, Czech Republic). All solvents, anhydrous sodium sulphate, and formaldehyde solution were purchased for Lach:Ner s.r.o., (Neratovice, Czech Republic). Pyrogallol, polyvinyl pyrolidone, 2,2′-Azobis(2-methylpropionitrile) (AIBN), pyrocatechol, glycidyl methacrylate, ethylene glycol dimethacrylate (stabilised with 90-110 ppm monomethyl ether hydroquinone as inhibitor), haematoxyline, eosine, iron(III) nitrate nonahydrate, calcium nitrate tetrahydrate, magnesium chloride, copper acetate, ammonium iron(II) sulphate hexahydrate and manganese sulphate monohydrate were purchased from Sigma-Aldrich Ltd. (Prague, Czech Republic). The radioactive sodium iodide $Na^{125}I$ was purchased from MGP Ltd. (Zlín, Czech Republic). All chemicals were used without additional purifications.

Mice C57BL/6 were obtained from Velaz s.r.o (Prague, Czech Republic). Mice feed was provided by Altromin Spezialfutter GmbH (Lage, Germany). Normal epithelial rat cells from small intestine IEC-6 were purchased from Sigma-Aldrich Ltd. (Prague, Czech Republic). Isoflurane (Aerrane 100%) for anaesthesia was purchased from Baxter S.A. (Lessines, Belgium).

3.2. Instruments and used methods

Fourier transform infrared (FTIR) was measured on the Perkin-Elmer Paragon 1000PC spectrometer (Perkin-Elmer Inc., Waltham, USA) equipped with the Specac MKII Golden Gate single attenuated total reflection (ATR). (Perkin-Elmer Inc., Waltham, USA)

Elemental analysis was performed using the Perkin-Elmer Series II CHNS/O Analyzer 2400 (PE Systems Ltd., Wigan, United Kingdom).

The particle size measurements were done with Mastersizer 3000 (Malvern Instruments Ltd., United Kingdom).

The structure, particle size and morphology of the prepared materials was studied with scanning electron microscopy (SEM) Quanta 200 FEG (FEI Company, Hillsboro, USA). The samples were dried and coated with a thin layer of gold by sputter coater Desk II (Denton Vacuum, Moorestown, USA).

ICP-MS-MS measurements were conducted on Agilent 7700 in He mode (inert gas flow was 4.1 ml/min) (Agilent, Santa Clara, USA). Internal calibration was used (calibrated on control samples without the addition of the polymer).

The activity of organs in *ex vivo* biodistribution study was measured on VDC-404 (Veenstra Instruments, Joure, Netherlands).

Atomic absorption was measured on Perkin Elmer, model 3110 (Perkin-Elmer Inc., Waltham, USA). For the light source hollow cathode lamp that emits a spectrum specific to the measured element was used. External calibration was used.

Solid-state NMR spectra were measured with 11.7 T using a Bruker Avance 500 US/WB NMR spectrometer (Bruker, Billerica, USA) in 4-mm ZrO_2 rotors. The ^{13}C cross-polarization (CP) magic angle spinning (MAS) NMR spectra were measured at a spinning frequency of 11 kHz or 15 kHz respectively, a nutation frequency of $B_1(^{13}C)$ field of 62.5 kHz and a contact time of 1.5 ms with a repetition delay of 2 s.

The SPECT/CT imaging was performed on an ALBIRA PET/SPECT/CT system (Bruker Biospin, Ettlingen, Germany), equipped with 3 detector rings consisting of 8 detectors each. Animals anesthetised with isoflurane were placed in the prone position for image acquisition.

All experiments involving mice have been performed according to the corresponding legislative, Act on Experimental Work with Animals (Decrees No. 311/97; 117/87 and Act No. 246/96 of the Czech Republic), which is fully compatible with the corresponding European Union directives.

3.3. Polymers synthesis

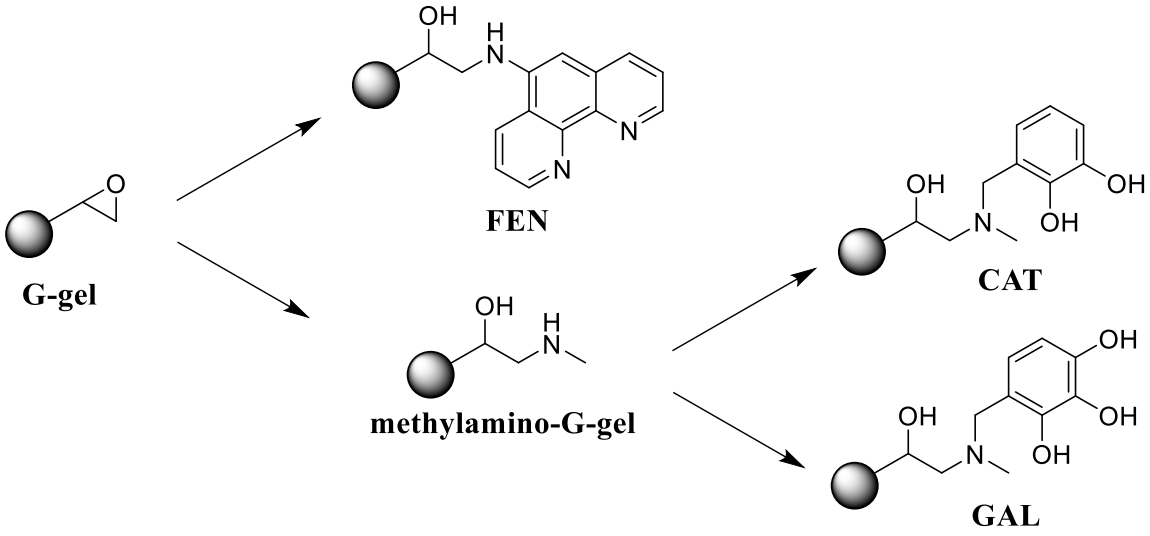

Figure 1: Scheme of polymer synthesis

3.3.1. Poly(glycidyl methacrylate-*co*-ethylene dimethacrylate) synthesis and characterisation (G-gel synthesis and characterisation)

A modified procedure according to (Švec F., 1975) was used: poly(*N*-vinyl pyrrolidone, M_W = 360,000 g/mol) (8.00 g, 22.2 μmol) and of sodium nitrite (0.40 g, 5.80 mmol) were dissolved in distilled water (400 mL) in a 1L round bottom flask. Afterwards, lauryl alcohol (98 g, 526 mmol), cyclohexanol (10 g, 100 mmol), ethylene glycol dimethacrylate (5.40 g, 5.1 mL; 27 mmol) glycidyl methacrylate (102.9 g, 95.7 mL; 725 mmol) and AIBN (0.50 g, 3.04 mmol) were added to the flask. The flask was subsequently flushed with nitrogen. The mixture was stirred vigorously at 70 °C for 2 hours followed by heating to 80 °C for 6 h. After the reaction, the mixture was filtered off, washed thoroughly with water, ethanol, methanol, diethyl ether and then dried on air.

The size of prepared particles was studied with Mastersizer 3000 (Malvern, Malvern, United Kingdom). The sample was dried and coated with a thin layer of gold by sputter

coater Desk II (Denton Vacuum, Moorestown, USA) and subsequently analysed by SEM (FEI Company, Hillsboro, USA).

FTIR (Figure S1): 2996 (w), 2938 (w), 1724 (s), 1480 (w), 1448 (w), 1390 (w), 1342 (w), 1252 (m), 1144 (s), 1132 (s), 1076 (m), 1060 (sh), 994 (m), 904 (m), 846 (m), 794 (w), 758 (m) and 536 (w) cm^{-1}.
^{13}C ssNMR (Figure S2; 126 MHz, ^{13}C CP/MS, NS = 2048, 11 kHz): δ 177.22, 67.44, 61.00, 54.95, 48.97, 44.62 and 16.38 ppm.
Elemental analysis: C 58.51 ± 0.11%; H 7.27 ± 0.02 %; N 0.12 ± 0.04 %

3.3.2. Poly[2-hydroxy-3-(*N*-methylamino)propyl methacrylate-*co*-ethylene dimethacrylate] synthesis (methylamino-G-gel synthesis)

G-gel (1.0 g, 6.70 mmol) and 40% aqueous methylamine solution (3.5 ml, 45 mmol) were added into 10 mL flask. The reaction mixture was stirred for 3 days at room temperature. Afterward, the polymer was filtered and washed thoroughly with PBS solution, 5% hydrochloric acid solution, water, ethanol, methanol, diethyl ether and then dried on air.

FTIR (Figure S3): 3300 (m; wide), 2940 (m), 2800 (s), 1720 (w), 1482 (w), 1448 (w), 1388 (w), 1252 (m), 1066 (w), 990 (wide), 944 (w), 874 (w) and 746 (w) cm^{-1}.
^{13}C ssNMR (Figure S4; 126 MHz, ^{13}C CP/MS, NS = 4096, 11 kHz): δ 177.45, 67.69, 54.58, 44.88, 36.28 and 17.46 ppm.
Elemental analysis: C 53.28 ± 0.00 %; H 8.60 ± 0.02 %; N 5.33 ± 0.07 %

3.3.3. Poly[2-hydroxy-3-(*N*-(2,3-dihydroxybenzyl)(*N*-methyl)amino) methacrylate-*co*-ethylene dimethacrylate] synthesis (CAT synthesis)

The methylamino-G-gel polymer (102 mg, 380 μmol), anhydrous sodium sulphate (680 mg, 4.80 mmol), pyrocatechol (70 mg, 636 μmol), methanol (1.5 mL) were added to a 25 mL flask. Then 40% aqueous solution of formaldehyde (0.375 mL, 5.44 mmol) was added in one portion, the flask was sealed and stirred with a magnetic stir bar at room temperature for 7 days. Afterward, the polymer was filtered and washed thoroughly with a portion of PBS buffer solution, 5% hydrochloric acid solution, water, ethanol, methanol, diethyl ether and then dried on air.

FTIR (Figure S5): 3372 (m), 2958 (m), 1720 (s), 1654 (w), 1455 (m), 1388 (m), 1256 (s), 1152 (s), 1056 (m), 958 (m), 870 (m), 856 (m) and 746 (m) cm^{-1}.
^{13}C ssNMR (Figure S6; 126 MHz, ^{13}C CP/MS, NS = 2048, 15 kHz): δ 177.89, 163.95, 145.35, 119.09, 64.33, 54.80, 34.42 and 18.56 ppm.
Elemental analysis: C 54.84 ± 0.13 %; H 7.77 ± 0.05 %; N 4.46 ± 0.01 %

3.3.4. Poly[2-hydroxy-3-(*N*-(2,3,4-trihydroxybenzyl)(*N*-methyl)amino) methacrylate-*co*-ethylene dimethacrylate] synthesis (GAL synthesis)

The polymer GAL was prepared by an analogous procedure as the polymer CAT, but pyrogallol (82 mg, 651 μmol) was used instead of pyrocatechol.

FTIR (Figure S7): 3388 (m), 2948 (m), 1720 (s), 1620 (m), 1452 (m), 1388 (w), 1252 (s), 1150 (s), 1056 (sh), 962 (m), 868 (m) and 750 (m) cm^{-1}.
^{13}C ssNMR (Figure S8; 126 MHz, ^{13}C CP/MS, NS = 2048, 11 kHz): δ 177.47, 144.14,

132.20, 118.43, 64.24, 55.68, 45.21, 34.47 and 18.32 ppm.
Elemental analysis: C 52.65 ± 0.01 %; H 6.67 ± 0.03 %; N 2.50 ± 0.02 %

3.3.5. Poly[2-hydroxy-3-(*N*-(1,10-phenanthroline-5-yl)amino)propyl methacrylate-*co*-ethylene dimethacrylate] synthesis (FEN synthesis)

G-gel (210 mg, 1.41 mmol), 1,10-phenanthroline-5-amine (900 mg, 4.61 mmol) and ethylene glycol (20 mL) were added to a 25 mL flask. The suspension was flushed with nitrogen, sealed and heated to 75°C while stirring for 3 days. Afterward, the mixture was washed with a portion of PBS solution, 5% hydrochloric acid solution, water, ethanol, methanol, diethyl ether and then dried on air.

FTIR (Figure S9): 3378 (m, wide), 2938 (m), 2886 (sh), 1722 (s), 1644 (w), 1482 (sh), 1448 (m), 1388 (w), 1252 (m), 1152 (sh), 1130 (s), 1062 (m), 990 (m), 840 (w), 792 (w), 748 (m) and 720 (w) cm^{-1}.
^{13}C ssNMR (Figure S10; 126 MHz, ^{13}C CP/MS, NS = 4096, 11 kHz): δ 177.28, 147.17, 132.10, 123.75, 67.23, 55.01, 48.97, 44.66 and 15.92 ppm.
Elemental analysis: C 52.58 ± 0.05 %, H 7.22 ± 0.04 %, N 1.65 ± 0.02 %

3.3.6. Synthesis of ^{125}I-labeled CAT polymer

To a 25 ml flask, G-gel (550 mg, 3.69 mmol), tyramine (20.0 mg, 146 μmol) and methanol (1.00 mL) was added. The mixture was stirred at room temperature for 1 day. The mixture was filtered and washed with water and methanol. The insoluble residue was added back to the flask with a 40% aqueous solution of methylamine (5.0 mL, 64 mmol). The suspension was stirred for 3 days, filtered, washed with water, ethanol, methanol and then dried.

In a 2 mL vial, 51.5 mg of this polymer and chloramine-T (10.0 mg, 44 μmol) were added to 400 μL of PBS. Then an aqueous solution of $Na^{125}I$ (373 MBq) was added. The mixture was stirred for 2 h. A fresh aqueous ascorbic acid was prepared (26 mg, 147 μmol in 1.00 mL of deionised water). After 2 hours a portion of this stock ascorbic acid solution (200 μL, 30 μmol) was added to the polymer. The mixture was centrifuged for 10 min, the supernatant was decanted and replaced with another portion of ascorbic acid solution (200 μL, 30 μmol) and with of PBS solution (1.00 mL). The mixture was stirred for 5 minutes and the polymer was washed two more times following the abovementioned procedure. The final washing was performed overnight with methanol, supernatant was decanted the polymer was washed twice with ultrapure water. The activity of the polymer after the filtration was 323 MBq, which corresponds to a decay-corrected radiochemical yield of 91%.

Finally, the polymer was reacted with formaldehyde and pyrocatechol according to a previously described CAT synthesis. The total activity of the polymer was 276 MBq corresponding with a decay-corrected radiochemical yield of 94 %. The overall radiochemical yield of the entire labelled polymer preparation was 86 %.

3.4. The calculation of concentration of functional groups

The molar amount x of investigated moiety per gram of each polymer was calculated. The results can be seen in table 2.

Formula 3 was used for the calculation of the molar amount of the epoxide moieties in the G-gel. It is based on the assumption that both glycidyl methacrylate and ethylene glycol dimethacrylate were equally reactive, hence their content in the polymer is equal to their corresponding molar ratio. The formula can then be written:

$$x_{\mathrm{GEL}} = \frac{\frac{m_{\mathrm{GMA}}}{m_{\mathrm{GMA}} + m_{\mathrm{EGDMA}}}}{M_{\mathrm{GMA}}} = \frac{\frac{V_{\mathrm{GMA}}\rho_{\mathrm{GMA}}}{V_{\mathrm{GMA}}\rho_{\mathrm{GMA}} + V_{\mathrm{EGDMA}}\rho_{\mathrm{EGDMA}}}}{M_{\mathrm{GMA}}} \quad (3)$$

Where $x_{\mathrm{MA-GEL}}$ is the molar amount of epoxide moiety per gram of polymer ($\mathrm{mol \cdot g^{-1}}$), m_{GMA} is the mass of glycidyl methacrylate (g), m_{EGDMA} is the mass of ethylene glycol dimethacrylate (g), M_{GMA} is the molar mass of glycidyl methacrylate in grams per ($\mathrm{mol \cdot g^{-1}}$), V_{GMA} and V_{EGDMA} are the volumes of glycidyl methacrylate and ethylene glycol dimethacrylate, respectively, added to the reaction flask ($\mathrm{cm^3}$) and ρ_{GMA} and ρ_{EGDMA} are the densities of glycidyl methacrylate and ethylene glycol dimethacrylate respectively ($\mathrm{g \cdot cm^{-3}}$).

Formula 4 was used for the calculation of the molar amount of the phenanthroline moiety in the FEN and the amine moiety in the methylamino-G-gel. It is based on the fact, that the investigated group concentration is directly proportional to the nitrogen content in the molecule. Since there was a minor nitrogen content in the G-gel polymer (possibly due to the nitrogen content in both the AIBN initiator and the sodium nitrite chain terminating agent), the nitrogen content in the G-gel was subtracted to give more accurate result. A formula for methylamino-G-gel can be written:

$$x_{\mathrm{MA-GEL}} = \frac{\omega_{\mathrm{N_{GEL-MA}}} - \omega_{\mathrm{N_{G-GEL}}}}{n_{\mathrm{N}} A_{\mathrm{N}}} \quad (4)$$

Where $x_{\mathrm{MA-GEL}}$ is the molar amount of the secondary amine moiety per gram of the polymer ($\mathrm{mol \cdot g^{-1}}$), $\omega_{\mathrm{N_{GEL-MA}}}$ is a mass concentration of nitrogen in methylamino-G-gel sample; $\omega_{\mathrm{N_{G-GEL}}}$ is a mass concentration of nitrogen in the G-gel sample; n_{N} is the number of nitrogens (in case of the FEN polymer n_{N} = 3 and in case of methylamino-G-gel n_{N} = 1) and M_{N} is the molar mass of nitrogen atom.

Formula 5 was used for the calculation of the molar amount of the chelating moieties in the CAT and the GAL. It is based on the fact, that the methylamino-G-gel contained nitrogen and that no additional nitrogen atoms were added to the polymer during the reaction. Thereafter the overall nitrogen content decreased after the reaction. The decrease of the nitrogen content is indirectly proportional to the number of chelating groups added to the polymer. The nitrogen content in G-gel was subtracted to give a more accurate result. The following equation can be written for the CAT polymer:

$$w_{\mathrm{CAT}} = 1 - \frac{\omega_{\mathrm{N_{CAT}}} - \omega_{\mathrm{N_{G-GEL}}}}{\omega_{\mathrm{N_{GEL-MA}}} - \omega_{\mathrm{N_{G-GEL}}}} \quad (5)$$

Where w_{CAT} is a mass fraction of the chelating moiety in the polymer, $\omega_{\mathrm{N_{CAT}}}$ is the observed content of nitrogen in the CAT sample, $\omega_{\mathrm{N_{G-GEL}}}$ is the mass concentration of

nitrogen in the G-gel sample and $\omega_{\mathrm{N_{GEL-MA}}}$ is the nitrogen content in methylamino-G-gel sample.

To get the molar amount of the chelating groups per gram of the polymer, we need to divide the molar mass of chelating groups. The molar mass of the chelating groups is directly proportional to the molar mass of the catechol and formaldehyde (which is a bonding group between the polymer and chelating group). The molar mass of water (which is eliminated during the reaction) needs to be subtracted. We then end up with the following equation for the CAT:

$$x_{\mathrm{CAT}} = \frac{1 - \frac{\omega_{\mathrm{N_{CAT}}} - \omega_{\mathrm{N_{G-GEL}}}}{\omega_{\mathrm{N_{GEL-MA}}} - \omega_{\mathrm{N_{G-GEL}}}}}{M_{\mathrm{CAT}} + M_{\mathrm{FA}} - M_{\mathrm{H_2O}}} \quad (6)$$

Where x_{CAT} is the molar amount of chelating groups per gram of polymer ($\mathrm{mol \cdot g^{-1}}$), $\omega_{\mathrm{N_{CAT}}}$ is the observed content of nitrogen in the CAT sample, $\omega_{\mathrm{N_{G-GEL}}}$ is the mass concentration of nitrogen in the G-gel sample and $\omega_{\mathrm{N_{GEL-MA}}}$ is the nitrogen content in the methylamino-G-gel sample, M_{CAT} is the molar mass of pyrocatechol ($\mathrm{g \cdot mol^{-1}}$), M_{FA} is the molar mass of formaldehyde ($\mathrm{g \cdot mol^{-1}}$), $M_{\mathrm{H_2O}}$ is the molar mass of water in grams per mol ($\mathrm{g \cdot mol^{-1}}$).

3.5. In vitro study

3.5.1. *In vitro* chelation study

For the measurement, ammonium iron(II) sulphate hexahydrate (245.5 mg, 0.6261 mmol) was dissolved in of ultrapure water (100 mL). The pH was adjusted with hydrochloric acid to 2.00 and 4.00, respectively. One millilitre of this solution was added to the chelating polymer (10.00 mg) and stirred vigorously. After 2, 5, 10 and 25 minutes respectively, the polymer was filtered off and the supernatant was collected. To each supernatant 10% aqueous nitric acid was added (1.00 mL). The concentration was determined using AAS (model 3110, Perkin Elmer, Wiltham, USA).

Analogously a solution of iron(III) nitrate, hexahydrate was prepared (248.9 mg, 0.6160 mmol in 100 mL of ultrapure water) and the pH was then adjusted to 2.00. Subsequently the chelation kinetics was measured analogously to the abovementioned one.

All data were fitted with the Formula 7 using Origin 2019 (version 9.6.0.172, OriginLab Corporation, Northampton, USA).

$$m_{\mathrm{Fe}} = m_{\mathrm{max}} \cdot (1 - e^{-k \cdot t}) \quad (7)$$

Where m_{Fe} is the mass of the chelated iron per gram of the polymer by time (mg), $m_{\mathrm{Fe-max}}$ is the total chelation capacity of the iron per gram of the polymer (mg), k is the rate constant ($\mathrm{min^{-1}}$) and t is the time of chelation (min). The total chelation capacity and the rate constant were calculated (Table 3).

3.5.2. *In vitro* selectivity study

The polymer chelation selectivity was measured. Calcium nitrate, tetrahydrate (5.89 g, 24.95 mmol), copper acetate (2.12 mg,11.70 μmol), iron(III) nitrate, nonahydrate (57.9 mg,

14.30 μmol), of magnesium chloride (1.57 g, 7.71 mmol), magnesium sulphate, tetrahydrate (9.34 mg, 41.90 μmol) and zinc chloride (22.93 mg, 168.μmol) were dissolved in ultrapure water (500 mL). The pH was adjusted to 2.00 or 4.00 respectively by addition of hydrochloric acid. Then to this solution (50 mL), the chelating polymer (CAT, GAL, FEN, respectively; 13.6 mg) was added and the mixture was stirred for 72 hours. A control group was made analogously but no polymer was added. Afterward, the mixture was filtered, and metal concentrations were determined in the supernatant using ICP-MS-MS (Agilent 7700, Santa Clara, USA). Using Formula 8 the polymer selectivity for Fe^{3+} ion was calculated.

$$S_{\mathrm{x}} = \frac{c_{\mathrm{Fe}^{3+}_{\mathrm{control}}} - c_{\mathrm{Fe}^{3+}_{\mathrm{final}}}}{c_{\mathrm{x}_{\mathrm{control}}} - c_{\mathrm{x}_{\mathrm{final}}}} \cdot \frac{c_{\mathrm{x}_{\mathrm{final}}}}{c_{\mathrm{Fe}^{3+}_{\mathrm{final}}}} \tag{8}$$

Where $c_{\mathrm{Fe}^{3+}_{\mathrm{control}}}$ is the Fe^{3+} ion concentration in the control experiment ($\mathrm{mol \cdot dm^{-3}}$); $c_{\mathrm{x}_{\mathrm{control}}}$ is the investigated ion concentration in the control experiment ($\mathrm{mol \cdot dm^{-3}}$); $c_{\mathrm{Fe}^{3+}_{\mathrm{final}}}$ is the Fe^{3+} ion concentration after the absorption ($\mathrm{mol \cdot dm^{-3}}$) and $c_{\mathrm{x}_{\mathrm{final}}}$ is the concentration of the investigated ion in the solution after the absorption ($\mathrm{mol \cdot dm^{-3}}$). The result can be seen in the Table 2.

3.5.3. *In vitro* cytotoxicity

Cytotoxicity was tested on IEC-6 cells. The cells were grown in full DMEM supplemented with insulin (0.1 $\mathrm{U \cdot mL^{-1}}$). Cell lines were maintained in a humidified atmosphere containing 5 % CO_2 and 37 °C.

The fabricated beads biocompatibility was studied as follows. Each polymer (CAT, GAL or FEN, respectively; 400 mg) was mixed with ultrapure water (40.0 mL) in a 50 mL plastic tube. The suspensions were rotary-mixed (120 rpm, 25 °C) using an MX-RD-Pro instrument (DLAB Scientific Inc., Riverside, USA) for 24 or 48 h. Thereafter, the suspensions were filtered through a 0.22 μm PVDF syringe filters. Subsequently, a commercially available powder-adjusted DMEM was used for the preparation of double concentrated DMEM (2 × DMEM) containing FBS, penicillin, streptomycin, amphotericin B and $NaHCO_3$ at full DMEM-corresponding concentrations (see above). When samples used for the incubation with IEC-6 cells, 2 × DMEM was supplemented with insulin at the above-mentioned concentration. The solutions to be tested were then prepared by mixing equal volumes of both the water extracts and 2 × DMEM with subsequent filter-sterilisation (0.22 μm PVDF syringe filter). The cytotoxicity was then studied by the methylthiazolyldiphenyl-tetrazolium bromide (MTT) assay.

The MTT assay was performed using IEC-6 cells. The cells were seeded in 96-well plates at a concentration of 10 000 cells/well. After 24 h of incubation at 37 °C in 5 % CO_2, the cell culture medium was replaced with the samples to be tested (see above). After 24 h or 48 h of incubation, the medium was aspirated and the cells were incubated with MTT solution (50 μL, 1 $\mathrm{mg \cdot mL^{-1}}$ in PBS) for 2 h. Subsequently, the MTT solution was aspirated and DMSO (100 μL) was added. A Synergy H1 Hybrid Reader instrument (Biotek, Winooski, USA) was used to assess the cell viability via spectrophotometry at 570 nm. The results of the MTT assay were expressed as a percentage of the control value, which was considered to be 100 %. The analysis was performed using at least three separate experiments.

3.6. *In vivo* study

3.6.1. Proof of non-resorbability of the polymer *in vivo*

The entire portion of the ^{125}I-labelled CAT polymer (276 MBq, synthetized in 3.3.6.) was then suspended in ultrapure water (1000 µL). Four mice were administered approximately 200 µL of polymer suspension via a probe into their stomachs. The amount of activity per mouse ranged from approximately 50 MBq to 90 MBq. The polymer location was observed by Albira PET - SPECT - CT (Biospin Bruker, Ettlingen, Germany) for 58 h. Afterward, the exact biodistribution profile was determined *ex vivo* by measuring the activity in each organ (stomach, intestine, colon, kidneys, liver, heart, spleen, and lungs) and blood sample (300 µl) using ionisation chamber (VDC-404, Veenstra instruments, Joure, Netherlands).

3.6.2. *In vivo* proof of suppression of iron uptake by the co-administered polymer

Two types of mice feed, Altromin 1324 Velaz (maintenance diet) and Altromin C 1038 (low iron diet), were ground into a fine powder and mixed in ratio 1.000:14.142. Three portions of the feed mixture had the CAT (5.85 g per kg), the FEN (15.63 g per kg) or no polymer (control group) added to the feed mixture respectively. The mixtures were then moisturised, mixed thoroughly into a paste, formed into pellets and dried at approximately 55 °C overnight.

For the experiment, 24 mice C57BL/6, 8 weeks old female were randomly divided into 3 groups (n = 6 mice). Mice were fed with the prepared diets. Their weight, haematocrit and haemoglobin levels were monitored approximately every 4 to 7 days. During the first four blood samplings, 500 µL of blood was taken in order to lower bodily supply of iron. Every following blood sample had a volume of 50 µL.

On day 41 of the experiment animals were sacrificed and their kidney, hearts, stomachs, small intestines, colons, and spleens were inspected for any histological abnormalities and pathology, more details listed in 3.7.

Dean-Dixon's Q test was applied to reject outlier values and then statistical significance was examined using ANOVA test performed by Origin (version 9.6.0.172, OriginLab Corporation, Northampton, USA).

3.7. Histology

Stomach, small intestine (duodenum, jejunum, ileum), colon, liver, spleen, kidney, and heart from 9 mice (3 from the CAT-treated group, 3 from the FEN-treated group and 3 from the control group) were fixed in 10% buffered formalin and embedded in paraffin. Serial sections (5 µm) were subsequently prepared and stained with haematoxylin-eosin.

4. Result and discussion

4.1. Polymer synthesis and characterisation

Poly(glycidyl methacrylate-*co*-ethylene dimethacrylate) (the G-gel) has been prepared by a modified procedure according to (Švec F., 1975) via a suspension radical polymerisation of glycidyl methacrylate with ethylene glycol dimethacrylate as a cross-linking agent. The reaction mixture was stirred vigorously creating small spheres of cyclohexanol and monomers in water, giving the reaction mixture a milk-like appearance. The reaction was carried out in these small spheres of the organic phase. The sodium nitrite solution prevented spheres from sticking into larger clusters. This procedure ensured the preparation of sufficiently small spheres of the polymer (Figure 1).

The size of the particles was measured using MALS (Mastersizer 3000, Malvern, United Kingdom). The size of the particles ranged from 15 to 400 μm in size, the majority of them was in the range from 25 to 90 μm (Figure 1). To verify the particle shape SEM was involved (Figure 2) and we found out that the majority of particles are round spheres; only a few irregularities, such as clusters of particles were observed. No particles with sharp edges were observed. Since very small particles could possibly be absorbed from the GIT, round spheres with diameter 5 μm or more were required for the application. Spherical structures were expected not to damage cells of the GIT mechanically – sharp fragments might irritate the GIT cells. On the other hand, small particles insured fast chelation kinetics and high chelation capacity.

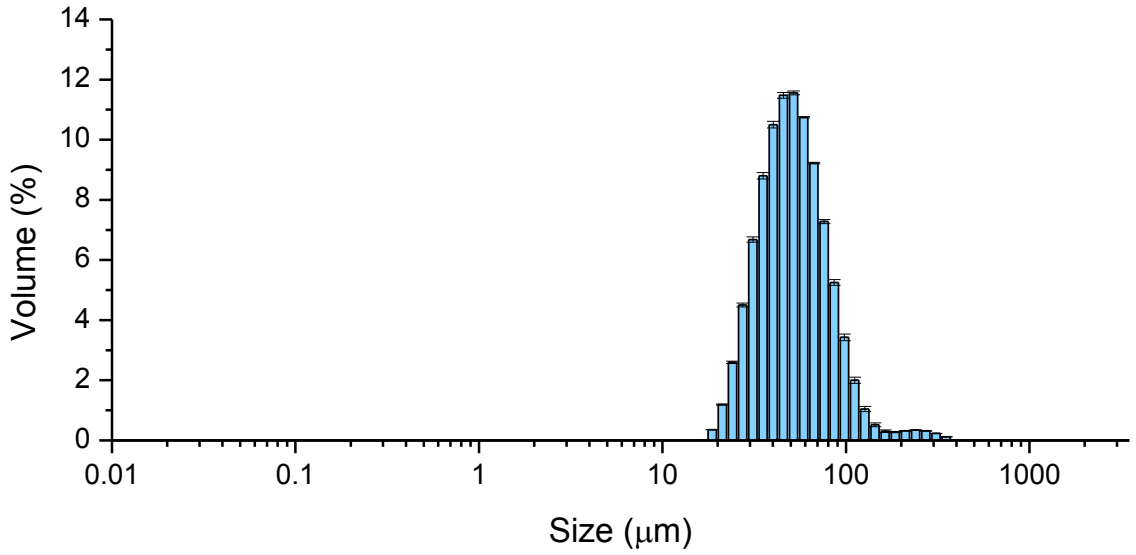

Figure 1: Histogram of particles size measured by MALS

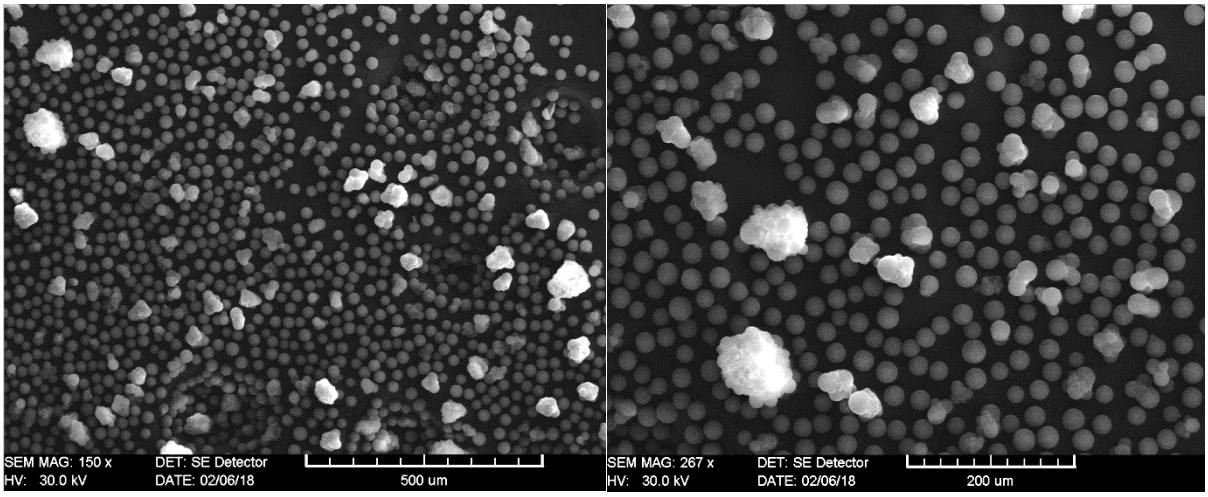

Figure 2: The scanning electron microscope (SEM) image of typical G-gel particles with two different magnification: 150 (left) and 267 (right), respectively. Only a few abnormalities (*e.g.* large clusters) other than round spheres can be seen.

The G-gel was characterised by FTIR and exhibited a strong band at 904 cm^{-1}, which is a typical signal of epoxide moiety presence, and at 1720 cm^{-1}, which is a typical region of the ester group (Figure S1). The ester group was confirmed by solid-state NMR, as the signal at 175 ppm (Figure S2).

The G-gel polymer was then reacted with methylamine solution. In this reaction, the epoxide ring was opened and a secondary amine was formed. FTIR has shown a significant decrease in the signal at 904 cm^{-1} corresponding to decreased epoxide group concentrations (Figure S3, Figure S11). The FTIR showed 3300 and 2800 cm^{-1} band, which are typical wavenumbers for hydroxyls and secondary amines. Solid-state NMR has also shown a significant decrease in 49 ppm signal (Figure S4). Compared to Figure S2, a new signal at 36 ppm has emerged, proving the methyl group presence.

The amine group in the methylamino-G-gel was then used for Betti reaction to covalently bind the chelating agent (pyrocatechol or pyrogallol) yielding the CAT and GAL polymers. The polymers were then washed very thoroughly with various solvents since there was a minor but still detectable amount of short non-crosslinked polymers which are soluble in water, in acidic or basic solutions. The purity of the polymer was determined by the UV-VIS absorption measurement of the supernatant. Once no significant absorption was detected in the range from 250 to 400 nm, the polymer was free of short polymer chains and used in other tests. Finally, the polymers were washed with 5% hydrochloric acid solution to remove alkali metal complexes and residues of PBS solution. FTIR has shown an increase of signal in the 1460-1480 cm^{-1} region corresponding to an aromatic ring presence (Figures S5, S7). The presence of aromatic carbons was further confirmed by a solid-state NMR in the range from 118 to 145 ppm (Figures S6, S8). Different reactant ratios (ratios of molar amounts of chelator:formaldehyde:G-gel of 1.0:5.7:1.0; 1.2:5.7:1 and 1.0:7.0:1.0) were tested; ratios presented in method had the greatest chelating capacities.

The FEN polymer was prepared in a different way than the CAT and the GAL. The 1,10-phenanthroline-5-amine was dissolved in ethylene glycol and was reacted at elevated temperatures with the epoxide groups in the G-gel. The reaction had a rather low yield,

possibly due both to steric hindrance of these relatively large chelating moieties and low nucleophilicity of the aromatic amine group. Ethanol, methanol, water, and ethylene glycol were tested as solvents; ethylene glycol has shown the best results. After the reaction, the mixture was washed thoroughly with several solvents as described with the CAT and the GAL polymers. FTIR has shown an increase of signal in 3378 and 2938 cm^{-1} area corresponding to the presence of hydroxyl and amine groups (Figure S9). Rather weak, but detectable signals were observed using the solid-state NMR in the range from 120 to 150 ppm which is typical for aromatic carbons (Figure S10).

While the GAL and the CAT were expected to form stable complexes with Fe^{3+} ions, the FEN polymer was expected to form a stable complex with Fe^{2+} ions. Since there is an equilibrium between Fe^{2+} and Fe^{3+}, decreased Fe^{3+} concentration due to stable complex formation leads to decreased Fe^{2+} concentration as well.

The *in vivo* biodistribution was analysed with the ^{125}I-labeled CAT polymer. The CAT polymer could not be labelled with radioactive iodine easily using a simple electrophilic iodination employing $Na^{125}I$ and chloramine-T, because it was expected that the *in situ* generated intermediates could oxidise catechol groups and the tracing would have only minor yields due to this side reaction; epoxide groups could also possibly decrease the yield, hence their presence was avoided during iodination. The G-gel was reacted with a small portion of tyrosine. The amount of tyrosine was less than 4% of the total amount of the epoxide groups in the reaction, which is still a significant excess to the amount of the radioactive iodine. Since the amount of tyrosine was minor, the physico-chemical properties were not expected to change significantly compared to the normal CAT polymer. Then the polymer was reacted with an excess of methylamine solution and subsequently labelled with the radioactive iodine ^{125}I in high yield. In the last step, the radioactive polymer was reacted with formaldehyde and pyrocatechol to forming the labelled CAT polymer.

The molar amount x of the investigated moiety per gram of each polymer was calculated using formulas 3, 4 and 6. The results are summarized in Table 2.

Polymer	x ($\mathrm{mmol \cdot g^{-1}}$)
G-gel	6.70
methylamino-G-gel	3.71 ± 0.09
CAT	1.37 ± 0.28
GAL	3.94 ± 0.19
FEN	0.367 ± 0.008

Table 2: The molar amount x of the investigated moiety per gram of each polymer, calculated via Formulas 3, 4 and 6.

4.2. *In vitro* chelation study

Aqueous solutions of Fe^{2+} salt and Fe^{3+} salts respectively were adjusted to pH 2.00, 4.00 and 6.00 respectively by addition of diluted hydrochloric acid. These conditions were supposed to represent a human stomach under different conditions. Solutions of Fe^{2+} salt solutions were prevented from oxidising on air by addition of ascorbic acid and they were kept under an inert atmosphere. The solution of Fe^{3+} ion at pH 4.00 was not stable in the long term: a precipitation of iron(III) hydroxide appeared soon upon preparation interfering with the chelation measurements. Only Fe^{2+} ion solutions at pH 2.00 and 4.00 and Fe^{3+} ion

solution at pH 2.00 were measured for chelation kinetics. A portion of the polymer was added to the solution and stirred for a period of time. There was an excess of iron ions in the solution (at least 2 folds the total chelation capacity of the polymer). After 2, 5, 10 or 25 minutes respectively the polymer was filtered, and the solution was analysed using AAS. The maximum chelating capacity of the polymer calculated with the Formula 7 and the results can be seen in the Table 1.

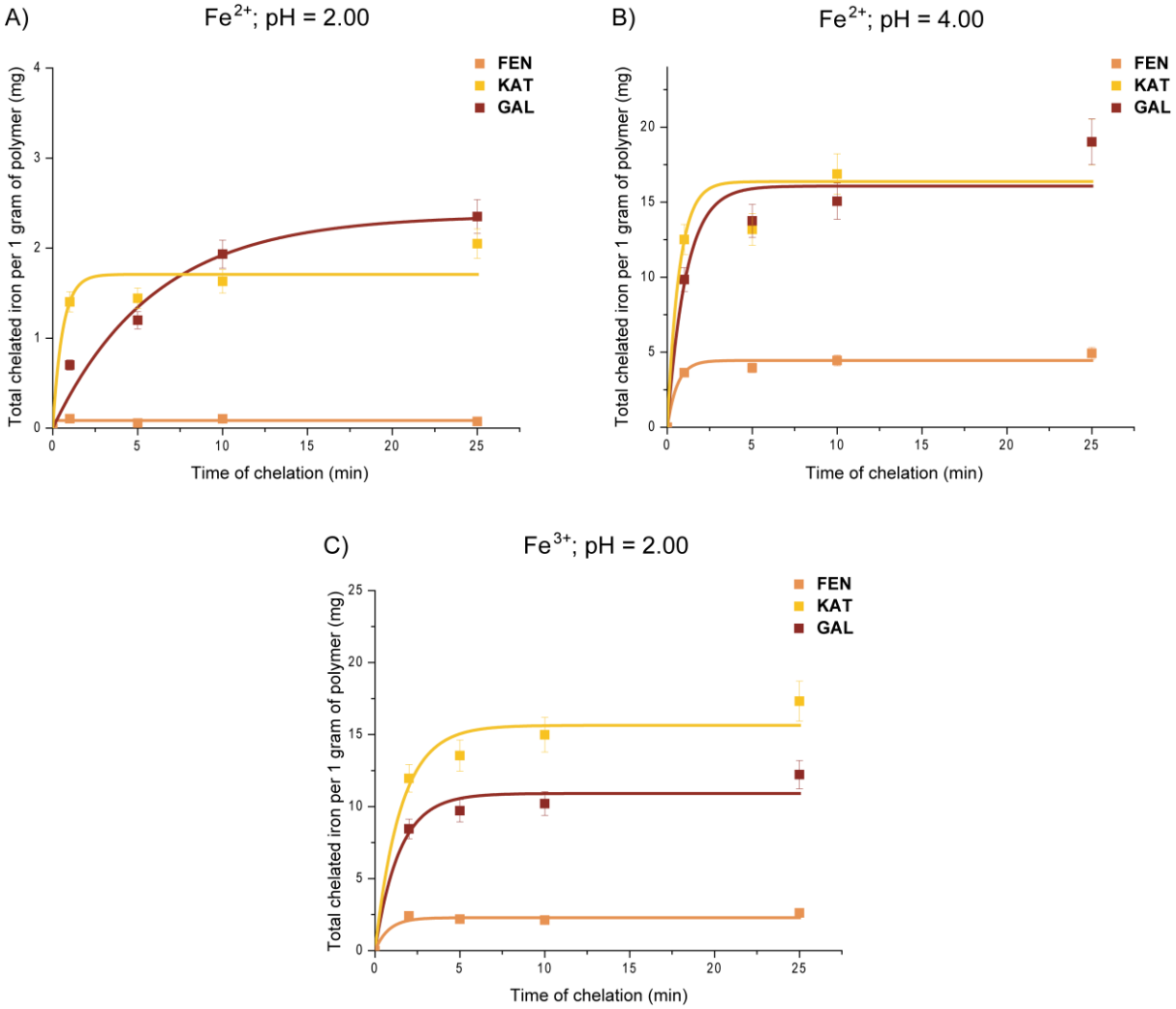

Figure 3: Iron absorption by the polymer as a function of time. A) Fe^{2+} ions at pH 2.00, B) Fe^{2+} ions at pH 4.00 and C) Fe^{3+} at pH 2.00.

As seen in the Figure 3, chelation of Fe^{2+} and Fe^{3+} ions is very fast, which is suitable for the proposed application. The chelation capacity for Fe^{2+} ion is noticeably higher at higher pH probably due to competition between metal complexation and protonation of the polymer-bound ligand.

Ion	Fe^{2+}				Fe^{3+}	
pH	2.00		4.00		2.00	
	m_{max} $(mg \cdot g^{-1})$	k (min^{-1})	m_{max} $(mg \cdot g^{-1})$	k (min^{-1})	m_{max} $(mg \cdot g^{-1})$	k (min^{-1})
GAL	1.7 ± 0.1	0.17 ± 0.05	16.1 ± 1.3	0.9 ± 0.4	10.9 ± 0.6	0.7 ± 0.2
CAT	2.3 ± 0.2	1.7 ± 0.9	16.4 ± 1.4	1.7 ± 0.5	15.6 ± 0.9	0.7 ± 0.2
FEN	0.085 ± 0.01	N/D	4.4 ± 0.2	1.4 ± 0.7	2.3 ± 0.1	N/D

Table 3: Fe^{2+} ion and Fe^{3+} ion chelation kinetics: m_{max} represents total chelation capacity, which is the total mass of iron absorbed by 1 gram of polymer, k is calculated rate constant of chelation. The values stated as N/D could not be determined with sufficient reliability.

4.2.1 *In vitro* selectivity study

Chelation selectivity was a major concern. In the *in vitro* chelation study, it was necessary to prevent the iron ions from precipitating out of the solution, since it would falsely increase the chelation capacity of the polymer. This was not an issue in the selectivity study, since we were interested only in the relative drop of the concentration in comparison to the control experiment (without the addition of the polymer).

A mixture of iron(III), magnesium, calcium, manganese(II), copper(II) and zinc salts in amounts and ratios relevant ton a typical diet were dissolved in water and the pH was adjusted with hydrochloric acid to values relevant to the human and mice stomachs. Then the CAT, the GAL, the FEN or no polymer (as a control experiment) was added; the iron ions were in at least 3 fold the stoichiometric excess to the maximum chelation capacity of the polymer. After the filtration, the ion concentrations in the supernatant were determined using ICP-MS-MS (Agilent 7700, Santa Clara, USA). Most ions other than iron were not absorbed and their concentration drop was within the statistical error. If a statistically significant drop of concentration was observed, chelation selectivity was calculated using the Formula 8. The results can be seen in the Table 4. The concentrations of each ion and their standard deviance can be seen in the Table S1.

Polymer	pH	Mg	Ca	Mn	Cu	Zn
FEN	2.00	*	*	*	< 0.01	*
FEN	4.00	*	*	*	< 0.01	10.4 ± 0.4
GAL	2.00	*	*	*	*	*
GAL	4.00	*	*	*	< 0.01	14.2 ± 2.1
CAT	2.00	*	*	*	*	*
CAT	4.00	*	*	*	8.2 ± 0.6	*

Table 4: Selectivity of Fe^{3+} ion chelation over Mg^{2+}, Ca^{2+}, Mn^{2+}, Cu^{2+} or Zn^{2+} ions was measured for each polymer. If the concentration drop after the chelation of any metal was statistically significant, a selectivity constant was calculated using the Formula 2 with the confidence level 95%. The * sign indicates no statistically significant ion concentration drop in the solution due to absorption was observed.

As seen in the Table 4, the polymer chelators exhibit a remarkable selectivity for Fe^{3+} ion over magnesium, calcium, manganese and zinc ions. The FEN polymer at both pH 2.00 and 4.00 as well as the GAL at pH 4.00, on the other hand, exhibited greater affinity towards

Cu^{2+} ions than towards Fe^{3+}. The GAL at the pH of 2.00 and the CAT at the pH of 2.00 and 4.00 exhibited only a minor affinity towards copper ion. The most selective polymer for Fe^{3+} chelation was the CAT with only a minor affinity to Cu^{2+} ions and negligible affinity to other ions.

4.2.2. *In vitro* cytotoxicity

Before performing the *in vivo* experiments we analysed the cytotoxicity by an MTT assay, as we wanted to ensure the safety of our beads-based formulation. Even though the prepared polymer beads were designed to be non-resorbable, a protracted release of water-soluble residues during the gastrointestinal passage represents a potential biocompatibility-related risk. Hence, the cytotoxicity study design was based on a modified ISO 10993-5 method (ISO 10993-5, 2009). This approach allowed us to test the potentially-released residues at a relevant concentration in a full DMEM by a common MTT assay.

The MTT assay results were evaluated as suggested by the ISO 10993-5 method (ISO 10993-5, 2009). In this method, a reduction of cell viability by more than 30 % is considered a cytotoxic effect. The testing was performed with epithelial rat cells from the small intestine (IEC-6), which is a suitable model for gastrointestinal toxicity (Thomas, et al., 2002), suggesting organ-relevant evaluation of possible cytotoxic effects.

Results from the cytotoxicity testing are shown in Figure 4. It is evident that all CAT-, GAL-based extracts caused no cytotoxic effects for IEC-6 epithelial, even when the extraction was performed for 48 h (GAL 48, CAT 48). In contrast, the FEN-based extracts caused a minor decrease in the viability of IEC-6, yet the effect was not strong enough for the polymer to be declared as cytotoxic. In reality, however, the gastrointestinal tract surface is protected by a luminal layer of mucins (Hansson GC., 2012) (Johansson M.E.V., 2013). This suggests that the real *in vivo* cytotoxic effects will be even lower and therefore negligible. This hypothesis was further confirmed by a robust histopathological examination (see 4.4.).

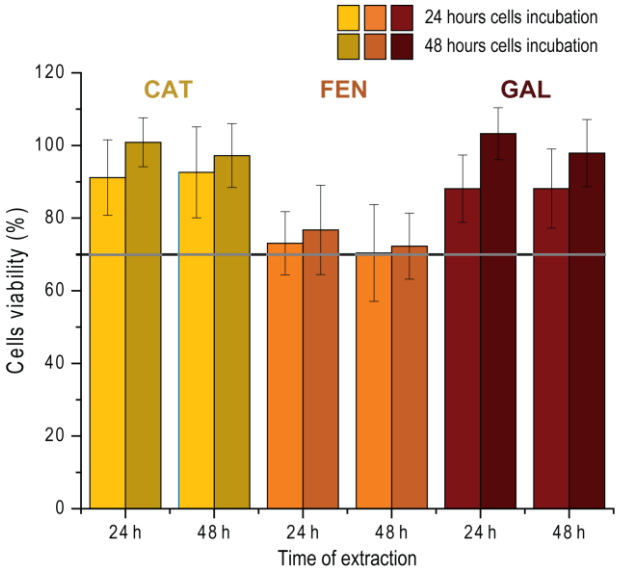

Figure 4: Cells viability assay (MTT assay). The polymers CAT, FEN and GAL were extracted in ultrapure water for 24 or 48 hours, respectively. Then IEC-6 cells were cultivated

in the extract for 24 hours or 48 hours, respectively. Grey horizontal line indicates the cytotoxicity threshold.

4.3. *In vivo* experiments

An experiment was conducted to prove that the prepared polymers have no biological availability from the GIT. Theoretically they should not be absorbed because of the particle size. Nevertheless, we needed to confirm this hypothesis and to find out the retention capabilities in the gastrointestinal tract. The *in vivo* biodistribution was tested with a ^{125}I-labeled CAT polymer. The biological distribution of the CAT, GAL and FEN polymers was expected to differ negligibly as their biodistribution is mostly size-determined and size of the microbeads is the same for all polymers (given by the same starting G-gel).

A suspension of the ^{125}I-labeled CAT polymer was administered to mice stomach (n = 4). SPECT and CT were used to visualise the location and concentration of the polymer in GIT. The merged SPECT and CT images can be seen in Figure 5, 35 min, 55 min, 4 hours, 8 h, 24 h, 46 h and 56 h, respectively, after radioactive polymer administration. In principle it would be possible to quantify the amount of polymer present in the organ according to the detected activity. ^{125}I emits mostly 27 keV X-rays and 35 keV gamma-rays (Katakura, et al., 1993), which have relatively low energies and therefore are absorbed by the surrounding tissue to a high extent. In other words, the total detected activity is heavily dependent on the geometry of the source (the shape of the organ) and the shielding of the surrounding tissue. SPECT images were therefore used merely as an illustrative spatial visualisation of the relative distribution within the body.

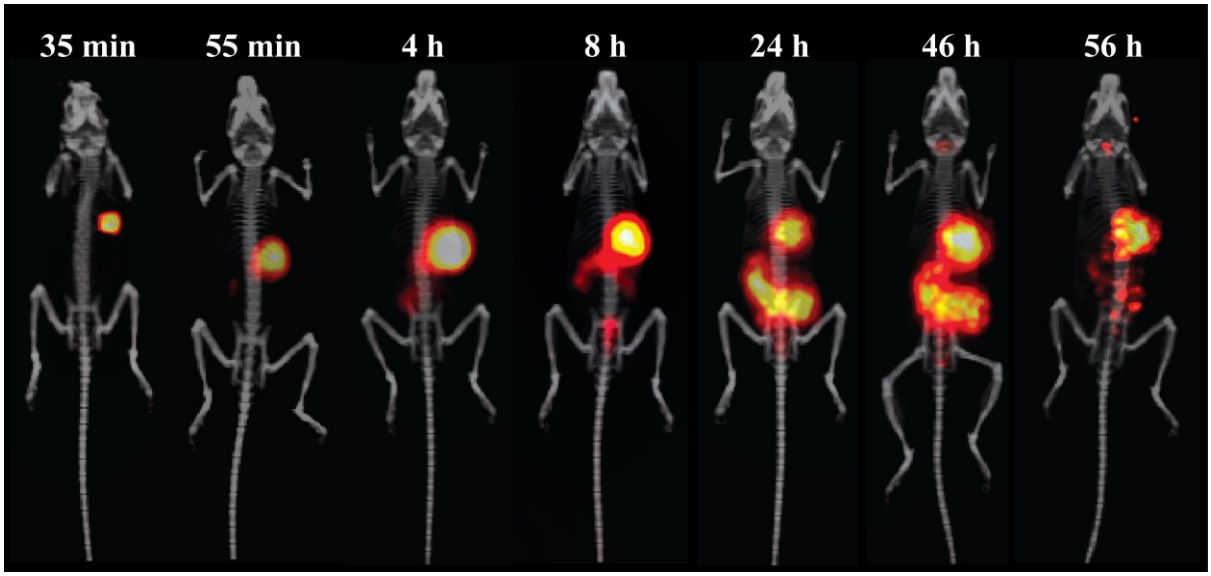

Figure 5: The merged images from SPECT camera and CT at 35 min, 55 min, 4 hours, 8 hours, 24 hours, 46 hours and 56 hours, respectively, after radioactive polymer administration. The activity is shown as a relative hotspot distribution in each frame.

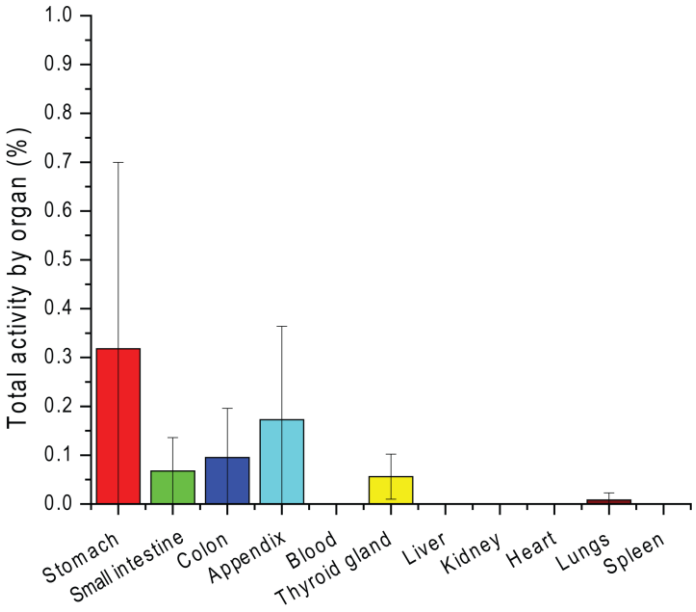

Figure 6: The total relative *ex vivo* activity (decay-corrected) in mice 58 hours after administration. The limit of quantification was 370 Bq or less than 0.001% of the administered activity. No activity was detected in the blood sample, liver, kidney, heart or spleen.

A minor activity was detected in the lungs of one mouse. This was probably caused by aspiration of the polymer during administration. A minor activity was also detected in the thyroid gland. This is probably due to polymer deiodination caused by deiodinase enzyme from bacteria present in the intestine of mice (Querido, 1956) (Häggblom M, 2003). Total activity found outside GIT was less than 0.1% of total activity administered. Excluding the already discussed thyroid gland and lungs, there was no detectable activity in any organ apart from GIT. This could, therefore, be a sufficient proof of non-resorbability of the polymer from the GIT.

The biological distribution data suggested that the polymer forms a depot in the stomach and is then slowly released. The biological half-life of the polymer (assuming it follows 1st order kinetics) was calculated to be 8.9 ± 2.5 hours in the stomach and 10.6 ± 2.7 hours in the entire GIT. This is very suitable for the intended application: the prolonged retention of the polymer in the stomach and GIT increases the time of absorption after a single *per os* administration increasing the efficacy. On the other hand, this increases the necessity of low toxicity and low pro-oxidative properties of the polymer to prevent any damage to the GIT over a long-term treatment.

The concentration of iron, copper, and zinc in both mice feeds (Altromin 1324 Velaz and Altromin C 1038) were determined by State Veterinary Administration of the Czech Republic (Státní veterinární ústav, Prague, Czech Republic). Used methods were consistent with the norm ČSN EN ISO/IEC 17025:2005 (EN ISO/IEC 17025, 2005) Altromin 1324 Velaz feed was found to contain 367.50 ± 40.42 mg of iron per kilogram, 11.60 ± 1.74 mg of copper per kilogram and 80.90 ± 12.14 mg of zinc per kilogram. Iron-deficient mice feed, Altromin, C 1038, was found to contain 9.70 ± 1.06 mg of iron per kilogram, 6.02 ± 0.90 mg of copper per kilogram and 27.60 ± 4.14 mg of zinc per kilogram. Both were ground into a

fine powder and they were mixed in weight ratio 1:14.142 to form a mixture with 35.00 ± 3.85 mg of iron per kilogram, which is recommended concentration of iron per kilogram (National Research Council (US) Subcommittee on Laboratory Animal Nutrition, 1995) and mimics the composition of common human diet. The final mixture was calculated to contain 6.41 ± 0.96 mg of copper per kilogram and 31.37 ± 4.71 mg of zinc per kilogram; which are all consistent with recommended mice feed values. (National Research Council (US) Subcommittee on Laboratory Animal Nutrition, 1995)

The mice were randomly divided into 3 groups and they were fed the prepared diets with the CAT polymer (chelator of Fe^{3+} ions), the FEN polymer (chelator of Fe^{2+} ions) or no polymer (the control group). The mice weight, haematocrit and haemoglobin levels were monitored. During the first four blood samplings, 500 μL of blood was taken every 5 to 7 days in order to lower the bodily supply of iron. Subsequently every 3 to 4 days a blood sample with volume of 50 μL was taken, which was sufficient for both the haemoglobin and the haematocrit levels determination, but it would decrease the iron blood levels only negligibly. Both the haemoglobin and the haematocrit levels were indicators of iron supplies in the body; the weight was an indicator of mice fitness (major pathologies could decrease the mice weights). This experiment was designed to reveal the efficacy of the polymer-based treatment and the sub-chronic toxicity.

On day 41 of the experiment animals were sacrificed and their kidney, hearts, stomachs, small intestines, colons, and spleens were inspected for any histological abnormalities and pathology, more details listed in 3.7.

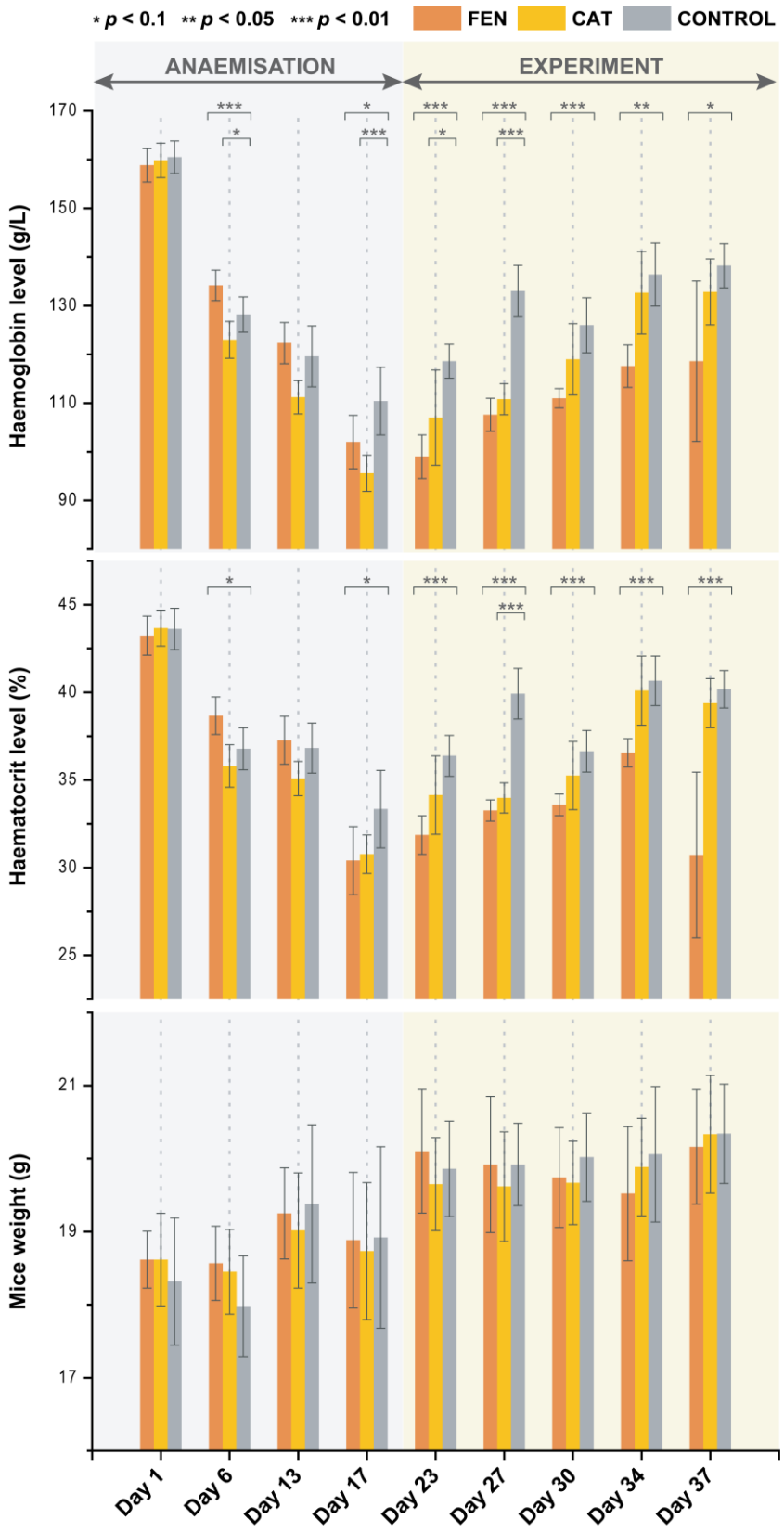

Figure 7: Comparison of haemoglobin levels, haematocrit levels and mice weight of all groups as a function of time

As expected, both haemoglobin and haematocrit levels decreased significantly during the first four 500 μL blood samplings. Within 10 days of the second phase of the experiment, the haemoglobin levels increased in control groups to a physiological level which was then maintained until the end of the experiment. In the FEN- and the CAT- treated groups, haemoglobin and haematocrit levels recovery were significantly slower. Moreover, particularly in the FEN-treated group the haemoglobin and haematocrit levels remained significantly decreased until the end of the experiment.

Because of the induced anaemia in mice, their erythrocytes were apparently both smaller in diameter and decreased in number. Therefore haematocrit levels were burdened with a greater error; making haemoglobin levels were more reliable marker of iron levels.

Both haemoglobin and haematocrit levels indicate that both the FEN and the CAT polymers decreased biological availability of iron from the feed. However, it is impossible to exactly quantify this effect, since an unknown amount of iron was stored inside the mice liver and spleen from the beginning of the experiment. These organ reservoirs of iron (though they were somewhat diminished after four phlebotomies) were one of the sources of iron for haemoglobin synthesis even if no iron was absorbed from the feed.

The FEN polymer exhibited a significantly greater efficacy despite having a lower chelation capacity (which was partially compensated by the increased FEN amount in the feed). This is possibly caused by the higher affinity of phenanthroline group towards Fe^{2+} ions which have a higher biological availability then Fe^{3+}. The Fe^{3+} ions chelation with the CAT polymer led to a statistically significant decrease of iron absorption, but the effect was weaker than with the FEN polymer. This indicated the necessity of the Fe^{2+} iron chelation to reach a proper therapeutic effect.

Before each blood sampling the mice weights were recorded. The weights in all groups slowly and steadily increased. There was neither a significant weight loss nor any other significant difference between groups of experimental animals.

4.4. Histology

Histological examination showed no difference between the control and polymer-treated animals. Neither specific pathological findings nor any distinctive changes in cytoarchitecture or tissue integrity were observed in the investigated samples of the stomach, small intestine (duodenum, jejunum, ileum), colon, liver, spleen, kidney, and heart showing local or systemic toxicity of the polymers.

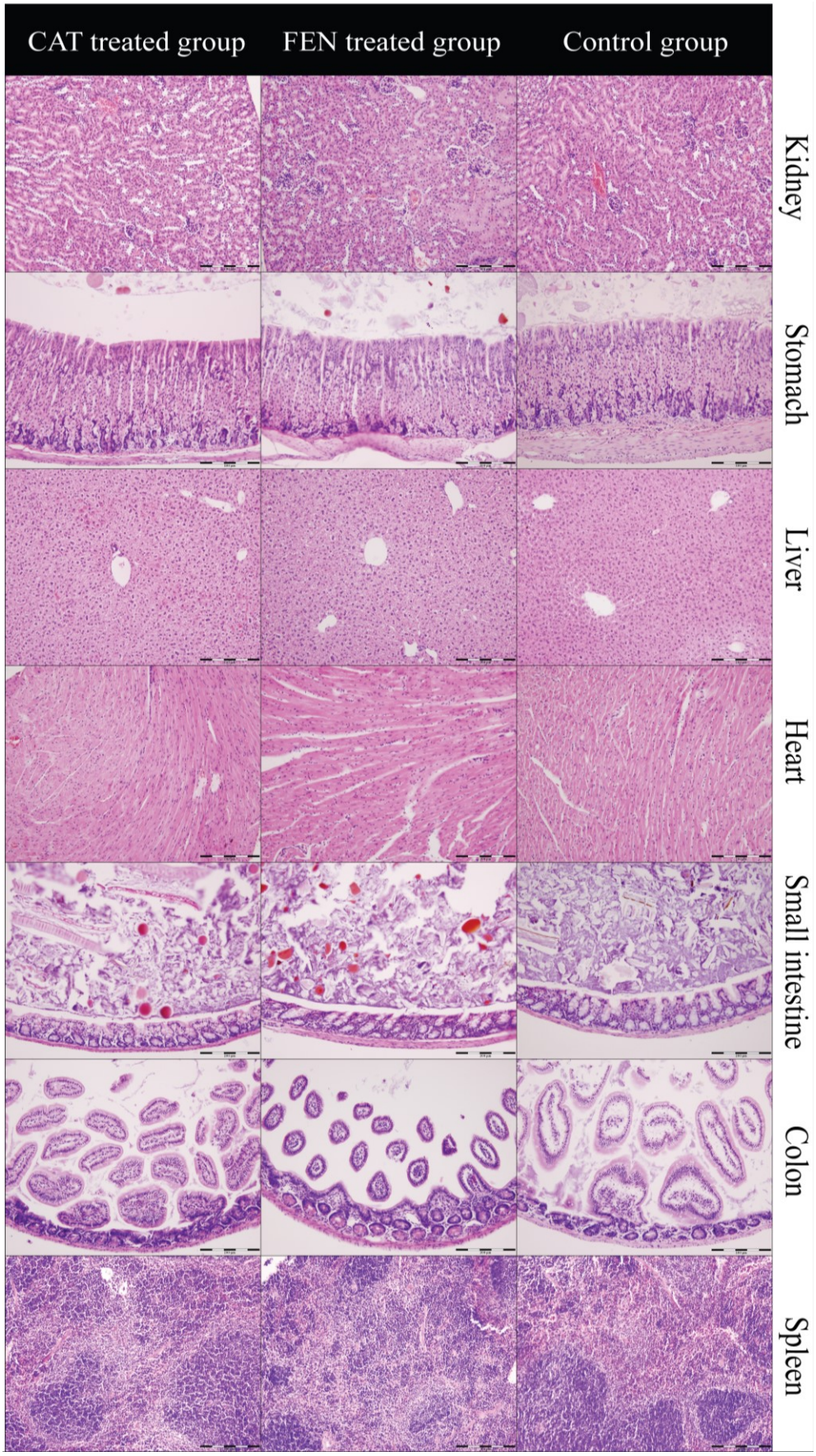

Figure 8: Organs histology of polymer-treated mice and control group after 41 days of continuous treatment. Stained with haematoxylin and eosin, magnification: 200.

5. CONCLUSIONS

A carrier polymer poly(glycidyl methacrylate-*co*-ethylene glycol dimethacrylate) (the G-gel) was prepared in the form of macroporous spherical beads ranging in size from 15 to 90 nm. This size of the beads was found to be sufficiently large to prevent absorption by the GIT but small enough to provide a reasonably large surface for iron absorption. These beads were then modified by epoxide ring opening reaction (the FEN and the methylamino-G-gel) or via the subsequent Betti condensation with formaldehyde and pyrocatechol or pyrogallol, respectively (the CAT and the GAL polymer respectively).

The CAT, the FEN and the GAL polymers were analysed for their absorption kinetics, maximum chelating capacities of each polymer and the chelation selectivity. They were shown to have a remarkably fast kinetics of sorption of both the Fe^{2+} and Fe^{3+} ions, which is suitable for the intended application. They were also shown to be remarkably selective for Fe^{3+} ions chelation over Mn^{2+}, Zn^{2+}, Ca^{2+} and Mg^{2+} ions. The CAT polymer was also a selective chelator for Fe^{3+} ions over Cu^{2+}.

All polymers were shown to be non-cytotoxic.

They were proven to have no *per os* biological availability, and did not cause any pathology in the gastrointestinal tract or any other organ in the daily sub-chronic *per os* administration.

Lastly, they were demonstrated to truly decrease the iron absorption from the feed. This decreased absorption was significantly more pronounced with the FEN polymer proving the necessity of Fe^{2+} ions chelation for a proper therapeutic effect.

Thus, we have successfully proven that it is possible to decrease the biological availability of iron from the gastrointestinal tract by addition of selective chelating polymers into the feed. Decreased biological availability of iron resulted in a decreased uptake, which in turn decreased the levels of haematocrit and haemoglobin.

The polymers presented in this study have applications in the treatment of chronic diseases caused by impairment of iron homeostasis leading to iron overload, such as haemochromatosis.

6. References

Adams P.C., and Barton J.C. 2007. Haemochromatosis. *Lancet.* 2007, pp. 370, 1855-60.

Bard, Allen J. 1985. *Standard Potentials in Aqueous Solution.* New York : Routledge, 1985. 9780203738764.

Becker, Johanna Sabine. 2002. Applications of inductively coupled plasma mass spectrometry and laser ablation inductively coupled plasma mass spectrometry in materials science. *Spectrochimica Acta Part B: Spectroscopy.* 57, 2002, Vol. 12, 1805-1820.

Brissot P., Ball S., Rofail D., Cannon H., and Wu Jin V. 2011. Hereditary hemochromatosis: patient experiences of the disease and phlebotomy treatment. *Transfusion.* 2011, pp. 51, 1331-1338.

Brissot P., Troadec M.B., Bardou-Jacquet E., Le Lan C., Jouanolle A.M., Deugnier Y., and Loréal O. 2008. Current approach to hemochromatosis. *Blood Reviews.* 2008, pp. 22, 195-210.

Bryszewska, Malgorzata Anita. 2019. Comparison Study of Iron Bioaccessibility from Sietary Supplements and Microencapsulated Preparations. *Nutrients.* 11, 2019, Vol. 2, 273.

Cappellini M.D., Cohen A, Piga A et al. 2006. A phase 3 study of deferasirox (ICL670), a once-daily oral iron chelator, in patients with beta-thalassemia. *Blood.* 2006, pp. 107, 3455-3462.

Debye, Peter. 1944. Light Scattering in Solutions. *Journal of Applied Physics.* 15, 1944, Vol. 338.

Eijkelkamp E.J., Yapp T.R., and Powell L.W. 2000. HFE-associated hereditary hemochromatosis. *Canadian Journal of Gastroenterology.* 2000, pp. 14, 121-125.

EN ISO/IEC 17025. 2005. General requirements for the competence of testing and calibration laboratories. *General requirements for the competence of testing and calibration laboratories.* 2005.

European Association For The Study Of The Liver. 2010. EASL clinical practice guidelines for HFE hemochromatosis. *Journal of Hepatology.* 2010, stránky 53, 3-22.

Fernández, Beatriz, Lobo, Lara and Pereiro, Rosario. 2019. Atomic Absorpton Spectrometry | Fundamentals, Instrumentation and Capabilities. *Encyclopedia of Analytical Science.* 3 edition, 2019, 137-143.

Flaten T.P., Aaseth J., Andersen O., and Kontoghiorghes G.J. 2012. Iron mobilization using chelation and phlebotomy. *Journal of Trace Elements in Medicine and Biology.* 2012, pp. 26, 127-130.

Fleming R.E., and Ponka P. 2012. Iron overload in human disease. *New England Journal of Medicine.* 2012, pp. 366, 348-59.

Galy B., Ferring-Appel D., Kaden S., Gröne H.J., and Hentze M.W. 2008. Iron regulatory proteins are essential for intestinal function and control key iron absorption molecules in the duodenum. *Cell Metabolism.* 2008, pp. 7, 79-85.

Greenwood, Norman and Earnshaw, Alan. 1997. *Chemistry of the elements.* Oxford : Butterworth Heinemann, 1997. 7506 3365 4.

Griffiths, PR. 1983. Fourier transform infrared spectrometry. *Science.* Oct 21, 1983, Vol. 222(4621), 297-302.

Griffiths, W.J.H. 2011. Haemochromatosis. *Medicine.* 2011, 39, 597-601.

Häggblom M, Bossert I. 2003. *Dehalogenation: Microbial Processes and Environmental Applications.* Boston : Kluwer Academic Publishers, 2003. 978-1-4757-7807-6.

Hála, Jiří. 2013. *Radioaktivní izotopy.* Tišnov : Sursum, 2013. 9788073232481.

Hansson GC. 2012. Role of mucus layers in gut infection and inflammation. *Current opinion in microbiology.* 2012, 15(1):57-62.

Hennel, Jacek W. and Klinowski, Jacek. 2004. Magic-Angle Spinning: a Historical Perspective. *New Techniques in Solid-State NMR.* 2004, volume 246.

Henter J.I., and Karlen J. 2007. Fatal agranulocytosis after deferiprone therapy in a child with Diamond-Blackfan anemia. *Blood.* 2007, pp. 109, 5157-5159.

Herman, Gabor T. 2010. *Fundamentals of Computerized Tomography.* Berlin : Springer, 2010. 1848828438.

ISO 10993-5. 2009. Biological evaluation of medical devices - Part 5: Tests for in vitro cytotoxicity. *Biological evaluation of medical devices - Part 5: Tests for in vitro cytotoxicity.* 2009.

Jervis, Kym E., Houk, Robert S. and Gray, Alan L. 1991. *Handbook of Inductively Coupled Plasma Mass Spectroscopy Handbook.* New York : Blackie, 1991. 0-216-92912-1.

Johansson M.E.V., Sjövall H., Hansson C.G. 2013. The gastrointestinal mucus system in health and disease. *Nature Reviews Gastroenterology & Hepatology.* 2013, 10, 352–361.

Katakura, J., et al. 1993. Nuclear Data Sheets for A = 125. *Nuclear Data Sheets.* 70, 1993, Vol. 2, 217-314.

Kondo H., Saito K., Grasso J.P., and Aisen P. 1988. Iron metabolism in the erythrophagocytosing Kupffer cell. *Hepatology.* 1988, pp. 8, 32-38.

Kupka, Karel and Šámal, Martin. 2007. *Nukleární medicína.* Praha : Grada, 2007. 978-80-903584-9-2.

Lima, Eduardo Vivaldo, et al. 1997. An Updated Review on Suspension Polymerization. *Industrial & Engineering Chemistry Research.* 36, 1997, Vol. 4, 939-965.

McMullan, Dominic. 1953. Scanning electron microscopy 1928–1965. *SCANNING.* 17, 1953, Vols. 175-185, 1995.

Morgan, John W. and Anders, Edward. 1980. Chemical composition of Earth, Venus, and Mercury. *Proceedings of the National Academy of Sciences of the United States of America.* 77, 1980, Vol. 12, 6973–6977.

National Research Council (US) Subcommittee on Laboratory Animal Nutrition. 1995. *Nutrient Requirements of Laboratory Animals: Fourth Revised Edition.* Washington (DC) : National Academies Press (US), 1995.

Navrátil, Leoš and Rosina, Josef. 2005. *Medicínská biofyzika.* Praha : Grada, 2005. 80-247-1152-4.

Pearson, Ralph G. 1963. Hard and Soft Acids and Bases. *Journal of the American Chemical Society.* 85, 1963, Vol. 22, 3533-3539.

Peters, Tim J., Raja, Kishor B. and Robert, James Simpson. 1992. Speciation of trace metals, with special reference to intestinal iron absorption. *Food chemistry.* 43, 1992, 315-320.

Pietrangelo, A. 2010. Hereditary hemochromatosis: pathogenesis, diagnosis, and treatment. *Gastroenterology.* 2010, pp. 139, 393-408.

Querido, A., Stanbury, J.B., Kassenaar A. A. H., Meijer J. W. A. 1956. The Metabolism of Iodotyrosines. III. Di-iodotyrosine Deshalogenating Activity of Human Thyroid Tissue. *The Journal of Clinical Endocrinology & Metabolism.* 1956, 16,8,1096–1101.

Remy, Heinrich. 1972. *Anorganická chemie.* Praha : Státní nakladatelství technické literatury, 1972. 04-604-72.

Roberts D.J., Brunskill S.J., Doree C., Williams S., Howard J., and Hyde C.J. 2007. Oral deferiprone for iron chelation in people with thalassaemia. *Cochrane Database of Systematic Reviews.* 2007, p. CD004839.

Schilt, Alfred A. 1962. Schilt, A. A. (1962). Mixed ligand complexes of iron(ii) as nonaqueous acid-base and aqueous oxidation-reduction indicators. *Analytica Chimica Acta.* 26, 1962, Vols. 134–143.

Simpson R.J., and McKie A.T. 2009. Regulation of intestinal iron absorption: the mucosa takes control? *Cell Metabolism.* 2009, pp. 10, 84-87.

Sood R., Bakashi R., Hegade V.S., and Kelly S.M. 2013. Diagnosis and management of hereditary haemochromatosis. *British Journal of General Practice.* 2013, pp. 63, 331-332.

Švec F., Hradil J., Čoupek J., Kálal J. 1975. Reactive polymers I. Macroporous methacrylate copolymers containing epoxy groups. *Die Angewandte Makromolekulare Chemie.* 1975, Vol. 1, 48.

Thomas, Carla and Oates, S. Phillip. 2002. IEC-6 Cells Are an Appropriate Model of Intestinal Iron Absorption in Rats. *Journal of Nutrition.* 132(4):680-7, 2002.

Worsfold, Paul et al. 2019. *Encyclopedia of Analytical Science.* Amsterdam : Elsevier, 2019. 978-0-08-101984-9.

Zimm, Bruno H. 1948. Apparatus and Methods for Measurement and Interpretation of the Angular Variation of Light Scattering; Preliminary Results on Polystyrene Solutions. *The Journal of Chemical Physics.* 16, 1948, Vol. 1099.

SUPPLEMENTARY DATA

S1. Selectivity study ions concentration data

Sample	pH	Mg (mg/L)	Mg SD	Ca (mg/L)	Ca SD	Mn mg/L	Mn SD	Fe (mg/L)	Fe SD	Cu (mg/L)	Cu SD	Zn (mg/L)	Zn SD
Control1	2.00	453.35	0.021	1149.0	0.021	2.5507	0.004	8.7390	0.008	0.96069	0.005	45.035	0.009
Control1	4.00	450.47	0.016	1146.7	0.021	2.5566	0.010	5.5973	0.013	0.95878	0.012	45.022	0.009
FEN	2.00	461.32	0.020	1164.1	0.019	2.5583	0.039	8.1487	0.041	0.00369	0.140	44.388	0.034
FEN	4.00	441.39	0.016	1115.7	0.016	2.4868	0.008	1.1926	0.028	0.00019	1.111	33.229	0.010
GAL	2.00	451.68	0.021	1146.2	0.025	2.5336	0.004	8.2473	0.017	0.95476	0.011	45.099	0.010
GAL	4.00	451.60	0.016	1150.9	0.016	2.5301	0.020	1.1829	0.029	0.00151	0.213	35.567	0.021
CAT	2.00	383.18	0.027	1054.9	0.029	2.3975	0.038	7.4136	0.039	0.85695	0.038	42.993	0.041
CAT	4.00	414.98	0.014	1141.5	0.009	2.5866	0.007	0.3189	0.011	0.70961	0.006	46.117	0.006
Control2	2.00	396.01	0.011	1090.7	0.011	2.4363	0.019	7.7548	0.025	0.87064	0.022	44.357	0.019
Control2	4.00	407.26	0.008	1130.1	0.013	2.5390	0.009	1.0135	0.024	0.89802	0.010	45.560	0.008

Table S1: Concentration of Mg^{2+}, Ca^{2+}, Mn^{2+}, Fe^{3+}, Cu^{2+}, and Zn^{2+} ions. Control1 is a solution equivalent to the one used in experiment with the FEN and the GAL polymers, while Control2 is a solution equivalent to the one used in the experiment with the CAT polymer. The concentrations were determined with ICP-MS-MS (Agilent 7700, Santa Clara, USA).

S2. FTIR and ssNMR spectra

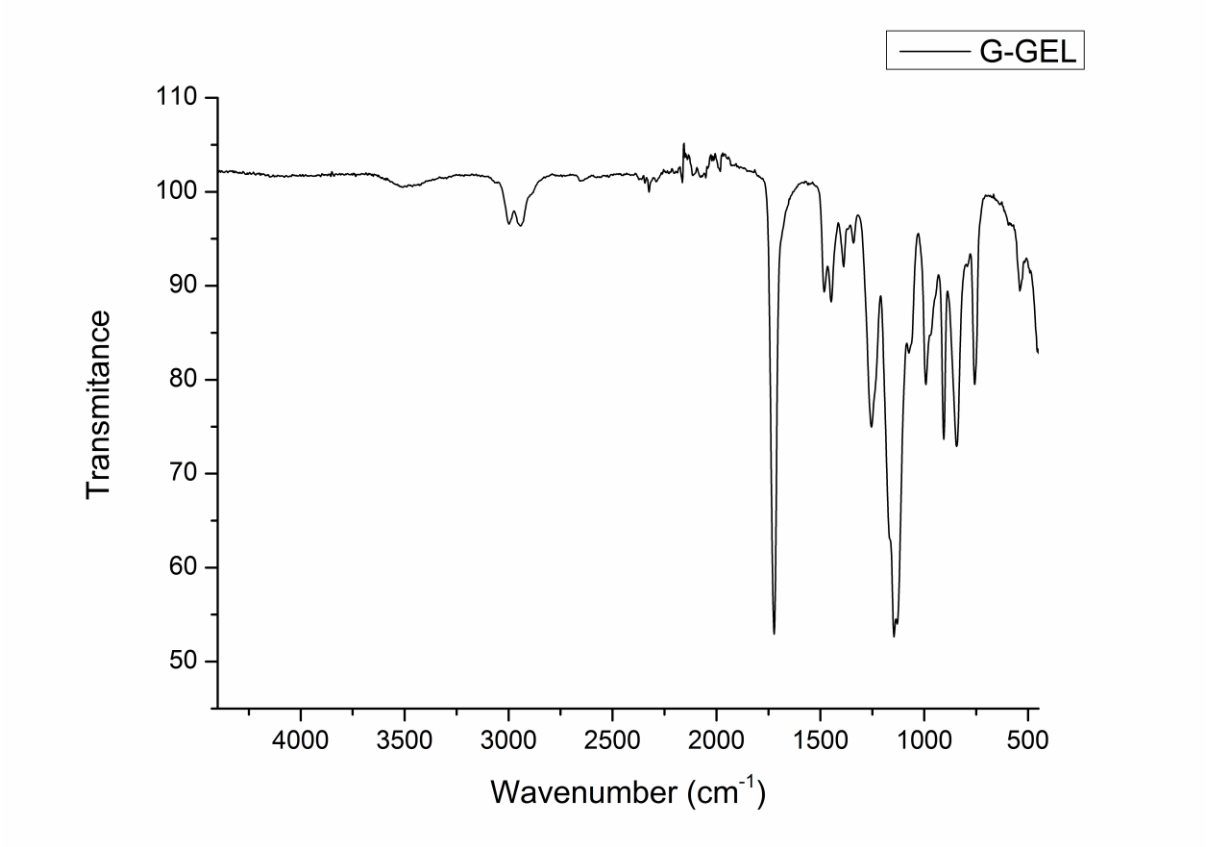

Figure S1: The G-gel IR spectrum

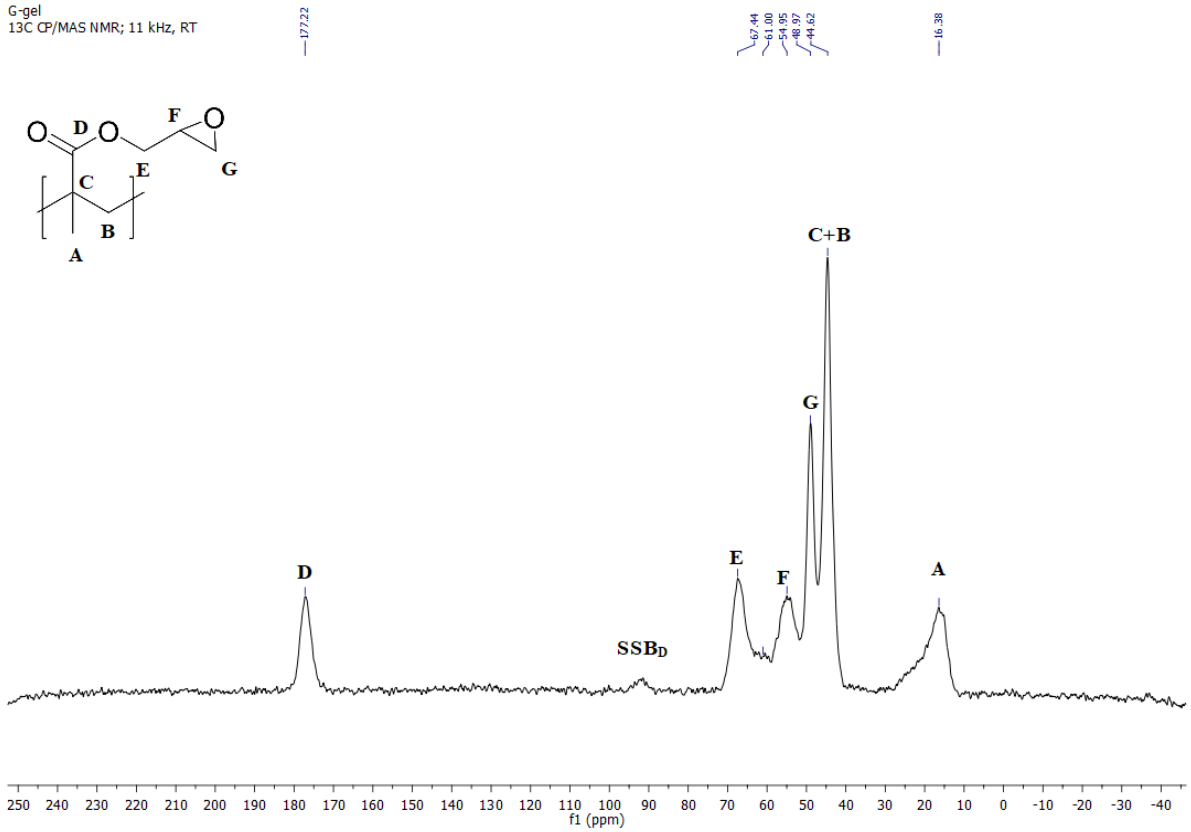

Figure S2: Solid state NMR spectrum of the G-gel. A solid sideband of D signal is noticeable (SSB_D)

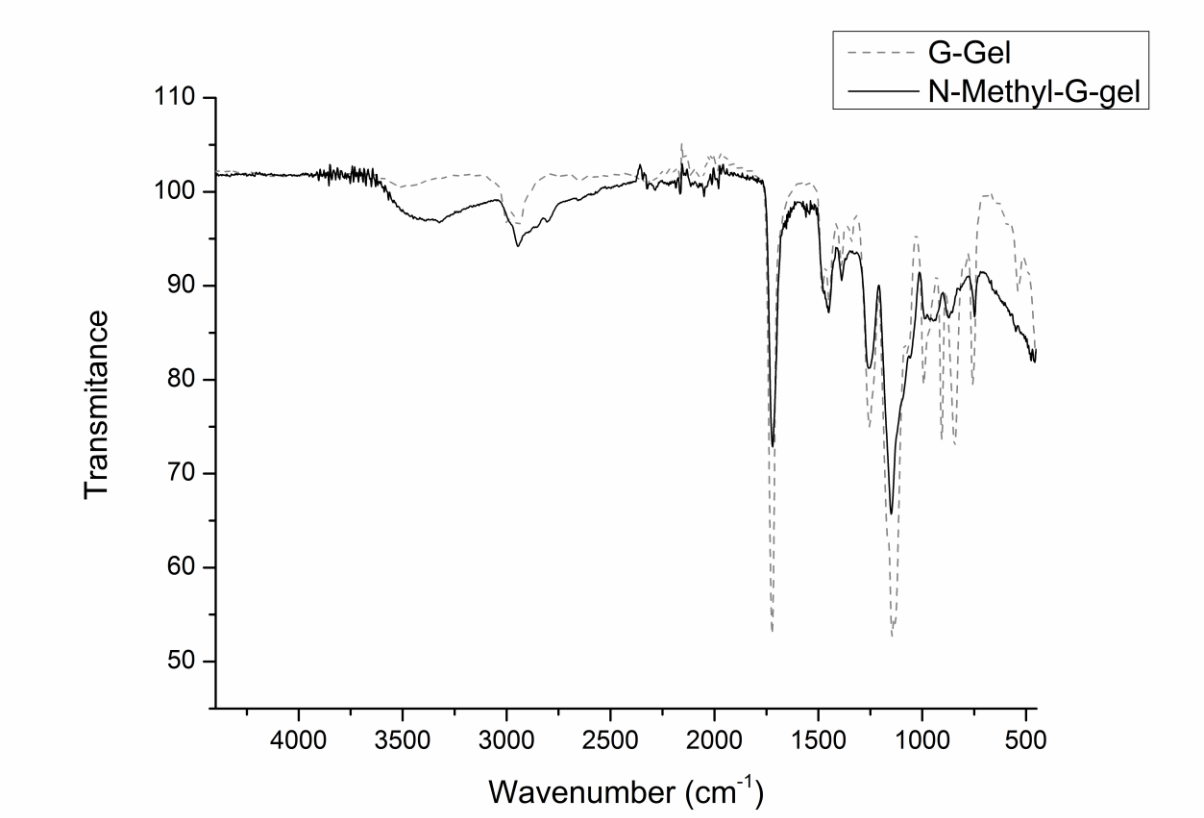

Figure S2: Comparison of the G-gel IR spectrum and the methylamino-G-Gel IR spectrum

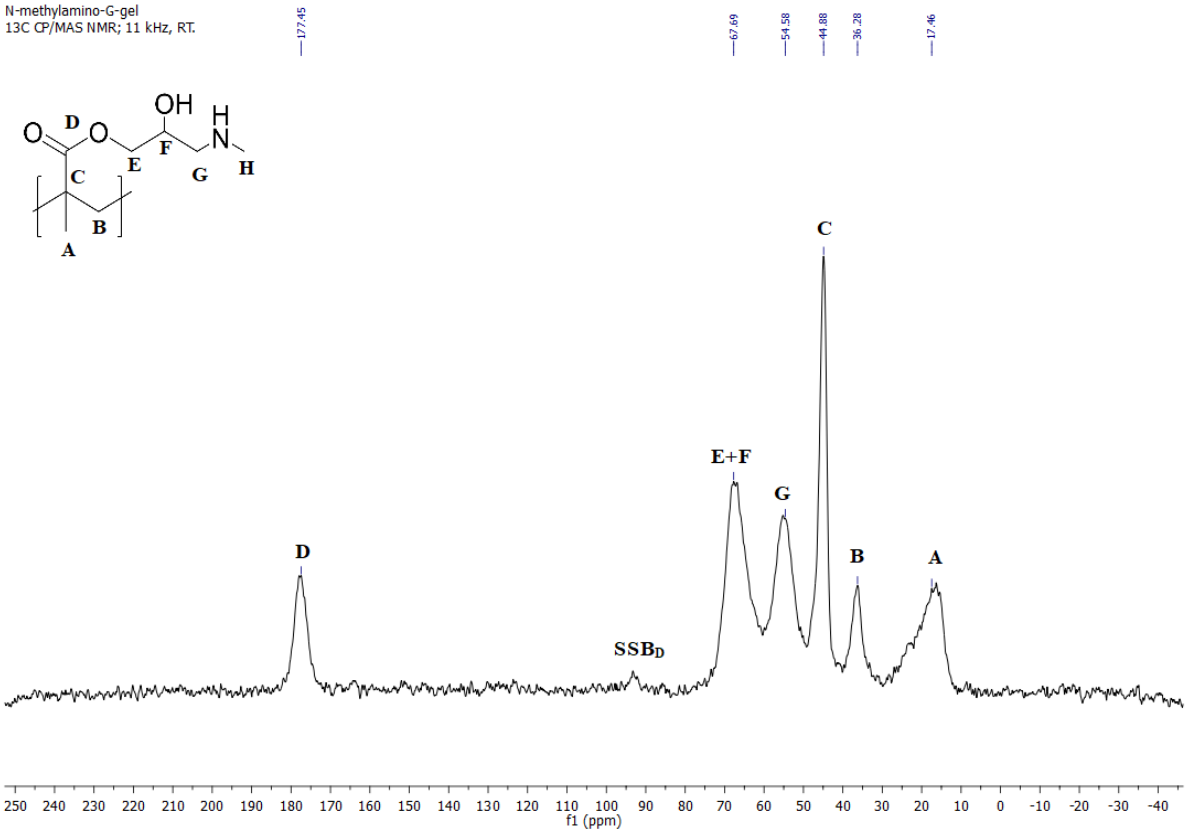

Figure S4: Solid state NMR spectrum of the methylamino-G-gel. A solid sideband of D signal is noticeable (SSB_D)

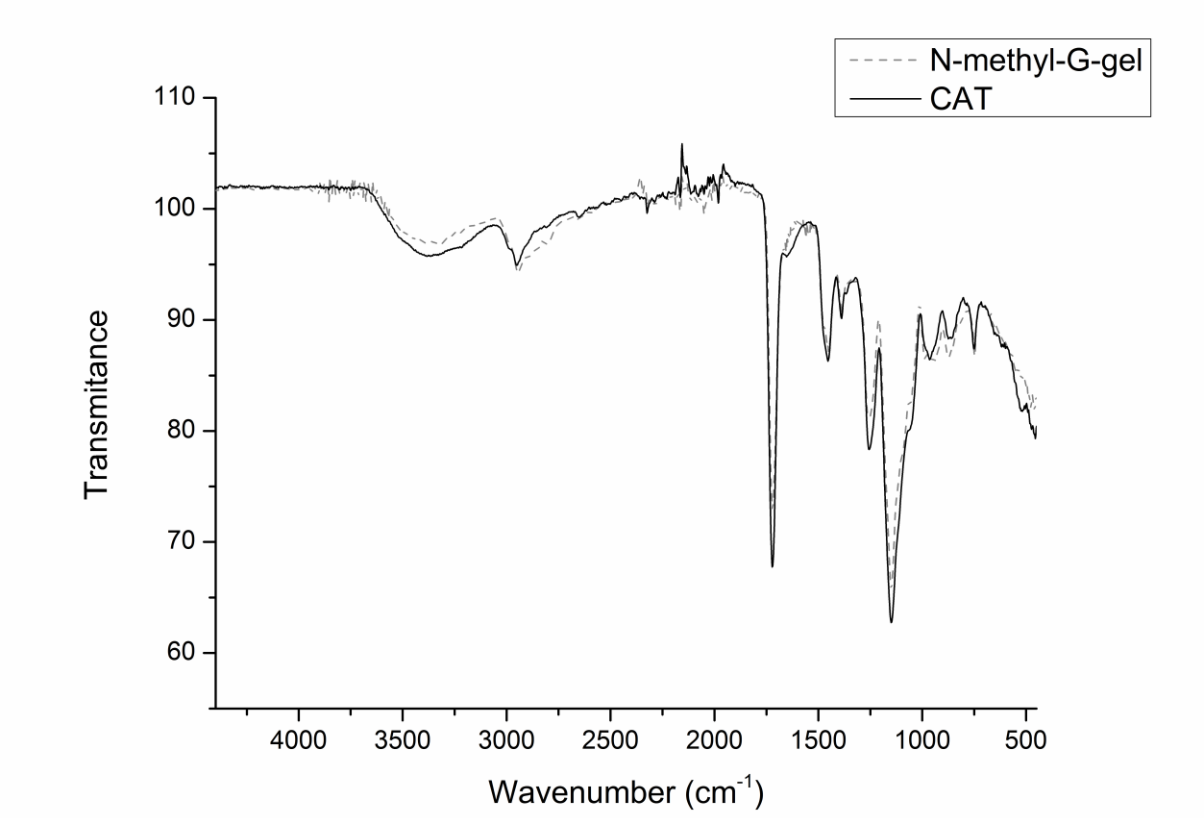

Figure S5: Comparison of Methylamino-G-gel IR spectrum and the CAT IR spectrum

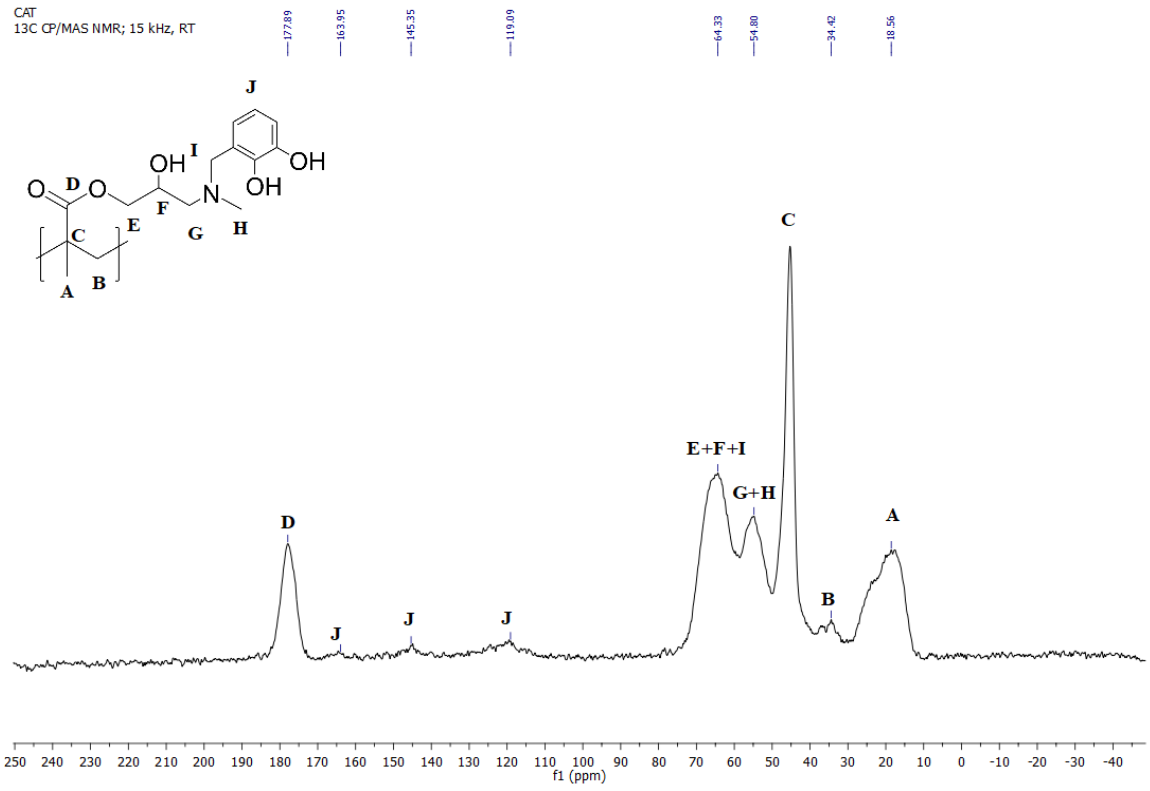

Figure S6: Solid state NMR spectrum of the CAT polymer.

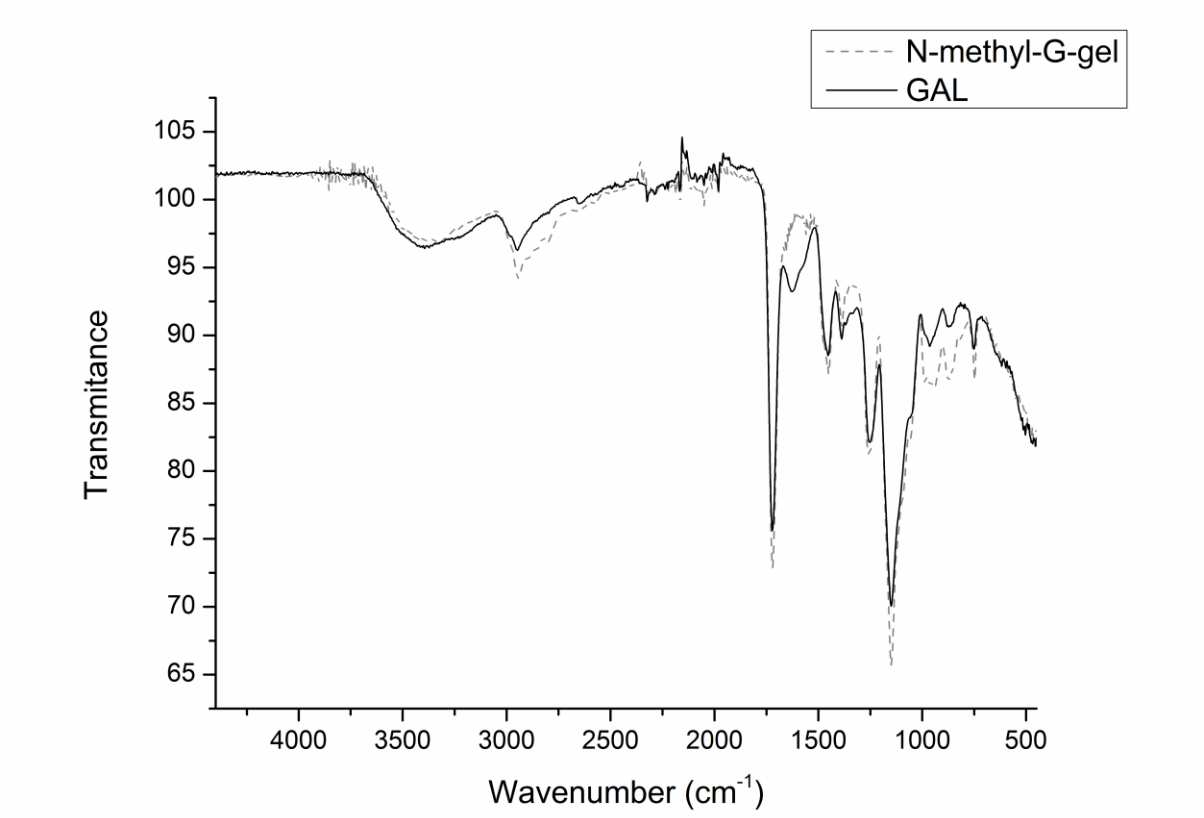

Figure S7: Comparison of the methylamino-G-Gel IR spectrum and the GAL IR spectrum

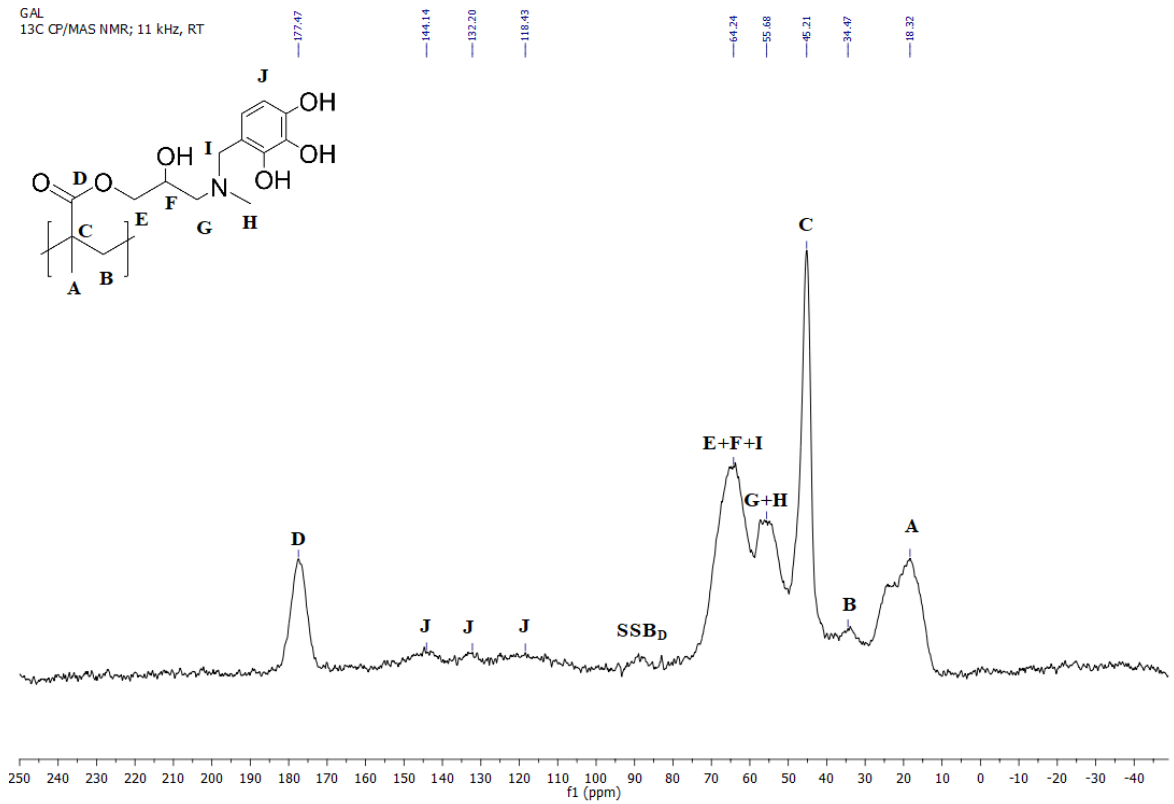

Figure S8: Solid state NMR spectrum of the GAL polymer. A solid sideband of D signal is noticeable (SSB_D)

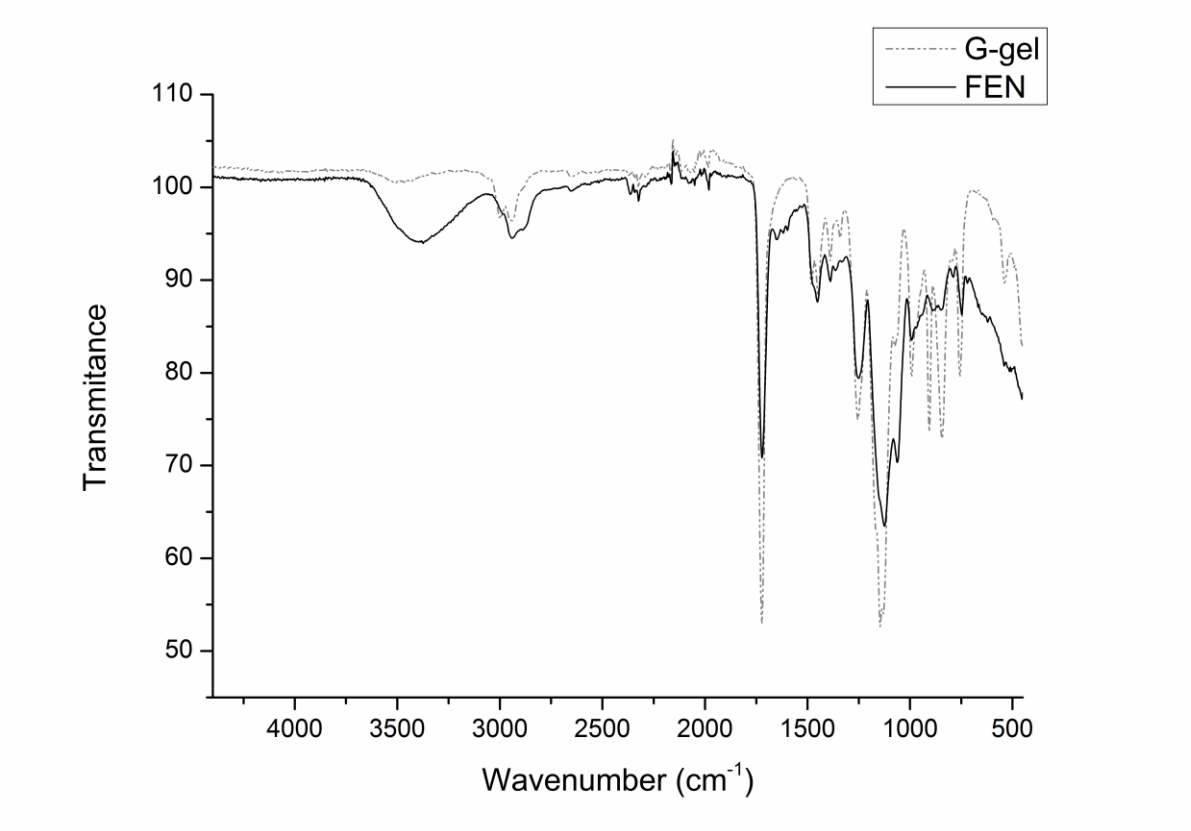

Figure S9: Comparison of the G-gel IR spectrum and the FEN IR spectrum

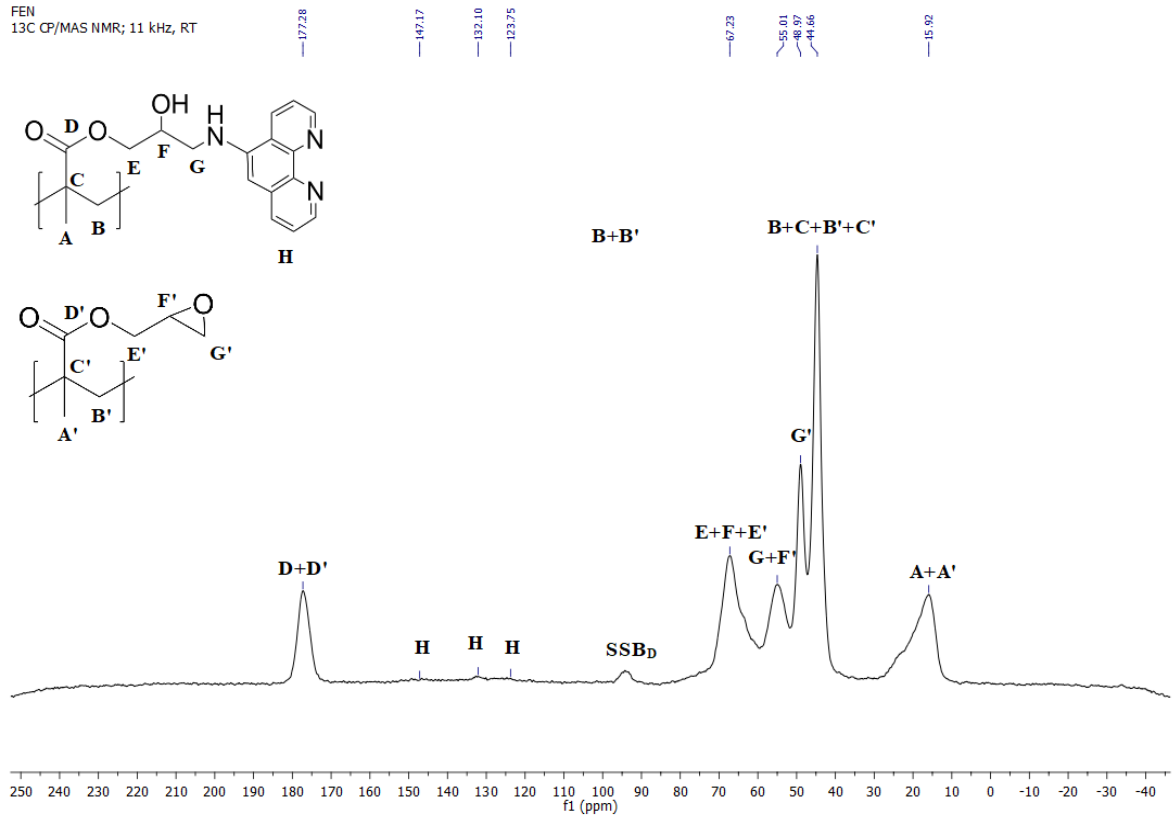

Figure S10: Solid state NMR spectrum of the FEN polymer. A solid sideband of D signal is noticeable (SSB_D)

S3. List of abbreviations

HSAB	hard and soft acids and base [theory]
AAS	atomic absorption spectroscopy
ICP-MS	inductively coupled plasma mass spectrometry
SEM	scanning electron microscopy
FTIR	Fourier transform infrared [spectroscopy]
SLS	static light scattering
MALS	multi-angle light scattering
(w)	weak
(m)	medium
(s)	strong
(vs)	very strong
(sh)	shoulder
NMR	nuclear magnetic resonance
CP	cross-polarisation
NS	number of scans
NMR	nuclear magnetic resonance
ssNMR	solid state nuclear magnetic resonance
MTT	methylthiazolyldiphenyl-tetrazolium [bromide]
AIBN	2,2′-azobis(2-methylpropionitrile)
PBS	phosphate saline buffer
GIT	gastrointestinal tract
aq	aqueous solution
Fc	ferrocene
Fc^+	ferrocenium ion
phen	1,10-phenanthrene
bipy	2,2’-bipyridine
edta	2,2’,2’’,2’’’-(ethane-1,2-diyldinitrilo)tetraacetic acid
quin	5-methyl-8-hydroxyquinoline
cat, CAT	benzene-1,2-diol
GAL	benzene-1,2,3-triol
FEN	5-amine-1,10-phenanthroline
DMEM	Dulbecco's modified eagle medium
M_W	molar weight

S4. Other data

Other chelating groups were tested, but were abandoned for various reasons. Poly(2-hydroxy-3*N*-(4-aminosalicylic acid)propyl methacrylate-*co*-ethylene dimethacrylate) showed remarkable affinity and selectivity, but the desired polymer was hard to obtain with sufficient chelation capacity. Poly(2-hydroxy-3*N*-(2-aminophenyl)propyl methacrylate-*co*-ethylene dimethacrylate), poly(2-hydroxy-3*N*-(3-aminophenyl)propyl methacrylate-*co*-ethylene dimethacrylate) and poly(2-hydroxy-3*N*-(4-aminophenyl)propyl methacrylate-*co*-ethylene dimethacrylate) were very poor chelators for iron, moreover 2-aminophenol and 4-aminophenol groups were chemically unstable and detectable amount of 2-benzoquinone and 4-benzoquinone, respectively, were detected after a period of storage time. Isocyanides were shown to have great affinity to iron and even to hem. Due to high reactivity resulting in storage instability and possible toxicity they were abandoned.